NTNU – Trondheim
Norwegian University of
Science and Technology

Design of Nacelle and Yaw Bearing for NOWITECH 10 MW Reference Turbine

Kristian Opsahl Bredesen

Master of Science in Mechanical Engineering
Submission date: February 2014
Supervisor: Bjørn Haugen, IPM

Norwegian University of Science and Technology
Department of Engineering Design and Materials

NORGES TEKNISK-
NATURVITENSKAPELIGE UNIVERSITET
INSTITUTT FOR PRODUKTUTVIKLING
OG MATERIALER

MASTEROPPGAVE VÅR 2013
FOR
STUD.TECHN. KRISTIAN OPSAHL BREDESEN

DESIGN AV NACELLE OG YAW LAGER FOR NOWITECH 10 MW REFERANSE TURBIN

Design of Nacelle and Yaw Bearing for Nowitech 10 MW Reference Turbine.

Utviklingen av vindturbiner har vært formidabel i de siste år. Det finnes kommersielt tilgjengelig 5 MW turbiner med diameter over 120 meter. Disse er også installert offshore på bunnfaste installasjoner. Morgendagens turbiner er muligens enda større og kan være flytende. Dette er et av temaene for forskningssentret NOWITECH. Det jobbes med å utvikle en referanseturbin på 10 MW som skal benyttes i forskningssammenheng på offshore flytende turbiner.

Oppgaven innebærer mekanisk design av en nacelle og rotor hub for en 10 MW offshore vindturbin .

Oppgaven bearbeides ut fra følgende punkter:

1) Litteratursøk
   a) Gjøre seg kjent med ”state of the art” av vind turbiner
   b) Gjøre seg kjent med design av vindturbiner og hvordan nacellen er dimensjonert
   c) Gjøre seg kjent med standarden IEC 61400

2) Software kjennskap
   a) Gjøre seg kjent med DAK-programmet NX
   b) Gjøre kjent med styrkeberegning vha Nastran
   c) Gjøre seg kjent med dynamisk analyse vha FAST og Fedem

3) Kontrollere mekanisk design med hensyn på utmatting for følgende komponenter:
   a) Bunnplate
   b) Hovedaksling
   c) Hub

4) Gjennomføre mekanisk design og dimensjonering av yaw-lager og overgang mot tårn.

Besvarelsen skal ha med signert oppgavetekst, og redigeres mest mulig som en forskningsrapport med et sammendrag på norsk og engelsk, konklusjon, litteraturliste, innholdsfortegnelse, etc. Ved utarbeidelse av teksten skal kandidaten legge vekt på å gjøre teksten oversiktlig og velskrevet. Med henblikk på lesning av besvarelsen er det viktig at de nødvendige henvisninger for korresponderende steder i tekst, tabeller og figurer anføres på begge steder. Ved bedømmelse legges det stor vekt på at resultater er grundig bearbeidet, at de oppstilles tabellarisk og/eller grafisk på en oversiktlig måte og diskuteres utførlig.

Senest 3 uker etter oppgavestart skal et A3 ark som illustrerer arbeidet leveres inn. En mal for dette arket finnes på instituttets hjemmeside under menyen masteroppgave (http://www.ntnu.no/ipm/masteroppgave). Arket skal også oppdateres en uke før innlevering av masteroppgaven.

Besvarelsen skal leveres i elektronisk format via DAIM, NTNUs system for Digital arkivering og innlevering av masteroppgaver.

Kontaktperson: Karl Merz, Nowitech

Roy Johnsen
Instituttleder

Bjørn Haugen
Faglærer

NTNU
Norges teknisk-naturvitenskapelige universitet
Institutt for produktutvikling og materialer

Abstract

NOWITECH (Norwegian Research Centre for Offshore Technology) are developing a 10 MW offshore reference wind turbine to encourage increased production of renewable energy. This thesis present a mechanical design and dimensioning of a transition piece between the yaw bearing (part of the nacelle) and the tower in this reference turbine. A fatigue analysis to verify the lifetime of 20 years for the main shaft, bed plate and transition piece has also been performed.

The final design has shape like a cone, which distributes the loads from the yaw bearing to the whole section of each tower leg. An extreme load case with 50 year occurrence period has been used for the Ultimate Limit State analysis. The material EN-GJS-400-18 is suggested for the transition piece, bed plate and main shaft. It has a yield strength of 240 MPa and a tensile strength of 370 MPa.

The mass of the transition piece is 49.6 tonnes and a peak stress of 262 MPa in a single node was found. This is further discussed in chapter 12.3 and 18.

The fatigue analysis was calculated with a detailed assessment described in the European standard, EN 13445-6 together with IEC 61400. The load case was calculated from Lars Frøyd's memo[1] with fatigue loads for power production. A static analysis in the software NX/Nastran was performed with conservative estimations. A damage factor for each load each was calculated and used to compute a total damage factor for 20 years.

The results confirmed the lifetime of 20 years for all parts despite all the conservative estimations (discussed in chapter 17 and 18).

Sammendrag

NOWITECH (Norwegian Research Centre for Offshore Technology) utvikler en 10 MW offshore referansevindturbin for å fremme produksjonen av fornybar energi. Denne masteroppgaven presenterer mekanisk design og dimensjonering av en overgang mellom yawlageret (i nacellen) og tårnet, i denne referanseturbinen. En utmattingsanalyse for å verifisere levetiden på 20 år er utført for hovedaksling, bunnplate og overgangen.

Den endelige utformingen av overgangen har form som en kjegle, som fordeler lastene fra yawlageret til hele tverrsnittet av hvert ben i tårnet. Et ekstremt lasttilfelle med en forekomst på en 50-årsperiode har blitt brukt i bruddgrensetilstandsanalysen for denne overgangen. Et materialet, EN-GJS-400-18 er foreslått for overgangen, bunnplaten og hovedakslingen. Det har en flytspenning på 240 MPa og bruddfasthet på 370 MPa.

Massen til overgangen er 49,6 tonn og en maximumsspenning på 262 MPa ble funnet i en enkelt node. Dette er diskutert i kapittel 12.3 og 18.

Utmattingsanalysen ble utregnet som en detaljert vurdering etter den europeiske standarden, EN 13445-6 og IEC61400. Lasttilfelle ble utregnet fra Lars Frøyds memo[1] med utmattingslaster fra produksjonstilstand. En statisk analyse i programmet NX/Nastran ble utført med konservative antagelser. En skadefaktor for hver last ble kalkulert og en total skadefaktor for 20 år ble funnet.

Resultatet bekreftet levetiden på 20 år for alle komponentene, tross alle de konservative antagelsene (disktutert i kapittel 17 og 18).

Contents

List of Figures

List of Tables

Acknowledgment

This thesis was carried out at the Norwegian University of Science and Technology (NTNU), Department of Engineering Design and Materials. The work was performed from October 2013 to February 2014 and the thesis has been submitted for the degree of Master of Science(MSc).

I would like to express my gratitude to Prof. Bjørn Haugen for his supervision, support and availability. He also presented this topic for me.

I wanted a task where I could learn modeling and simulation in NX and Nastran properly since my knowledge of this software is modest. In that context I would like to thank Magnus Skogsfjord, NXportalen who helped me with some difficult modeling.

I am grateful to Karl Otto Merz from NOWITECH for answering all my questions. I would also like to thank Daniel Zwick and Einar Agnalt who provided me with 3D-models and my 12 fellow office colleagues for helping me with various tasks.

Special thanks to Gunnar Härkegård for several interesting lectures and help through the course TMM4195 Fatigue Design, that I participated in fall 2013 to increase my knowledge about fatigue design used in this work.

Finally I wish to express my deepest gratitude to Elen Katrine Skjerve, my friends and family for invaluable support through these years at NTNU.

Trondheim, February 2014

Kristian O. Bredesen

Kristian Opsahl Bredesen

1 Introduction

A wind turbine is a device that converts kinetic energy from the wind into electrical current.[4]

1.1 General Background

Wind has been used as an energy resource for over 1000 years. The purpose at that time was milling of grains and pumping water. Since the discovery of electricity, the purpose of wind energy has changed. Many ways of converting wind to energy has been tried, but now the horizontal tower wind turbine are the most frequently used. In June 2013 the total wind capacity in the world was 296255 MW according to the World Wind Energy Association[5].

For increased average wind speed, the wind turbines can be placed offshore. Here the wind reach about 90% higher speeds than in the inland, and there are no turbulence due to topography.[3]

There are also several other benefits with offshore wind turbines. For instance there are no need for roads or other infrastructure and no or less visual pollution. There are also a lot of new challenges like exposure of seawater, waves, water depth and soil conditions.

1.2 Goal

There are two main goals for this thesis:

1. To design and dimension the transition piece between the yaw bearing and the tower with regard to calculated maximum stress, weight and guidelines from relevant standards.
2. Perform a fatigue analysis of the top of the wind turbine, including the hub, main shaft and the bed plate to verify the lifetime of the structure.

1.3 Scope of Work

The thesis will start with a short introduction of wind turbines in general and the NOWITECH turbine. Then the applied theory will be presented before the design process of the transition piece is shown in part 1. Here, the method of designing and building the model and the set up of the simulation in NX 8.5 will be explained. After that the results and comments for the ultimate limit state (ULS) analysis of the transition piece are presented.

In part 2, the procedure of the Fatigue Limit State (FLS) analysis is shown including use of standards, calculations, and assumptions made before the results and comments are presented. Finally discussion, conclusion, and some proposals for further work is given.

2 NOWITECH 10 MW Reference Wind Turbine

NOWITECH or Norwegian Research Centre for Offshore Technology wish to create a reference wind turbine that students and companies can use to compare their work to. In that way they can encourage to a increased use of wind power. The project is a cooperation between NOWITECH and NTNU were many PhD candidates and master students from different engineering disciplines are participating.

The reference turbine is a 10 MW, up wind, horizontal axis wind turbine with a diameter of 141 meter and a height of 164 meter above sea level. The reference turbine is chosen to be a direct drive turbine (no gearbox) and the blades are made of a combination of glass fiber and carbon fiber.

The reference site is chosen to be the K13 Alpha weather station (see figure 1), where the average wind speed at 90 meters above sea level is 10 m/s. This represent the conditions of wind turbine placement on the Dogger Bank in the North Sea.

Figure 1: K13 Alpha Weather station (53°13”04’N and 3°13”13’E) [2]

The main structural parts missing in this project is the generator (rotor and stator) and the transition piece between the tower and nacelle. The weight of the rotor and stator are specified and included in table 2.1.

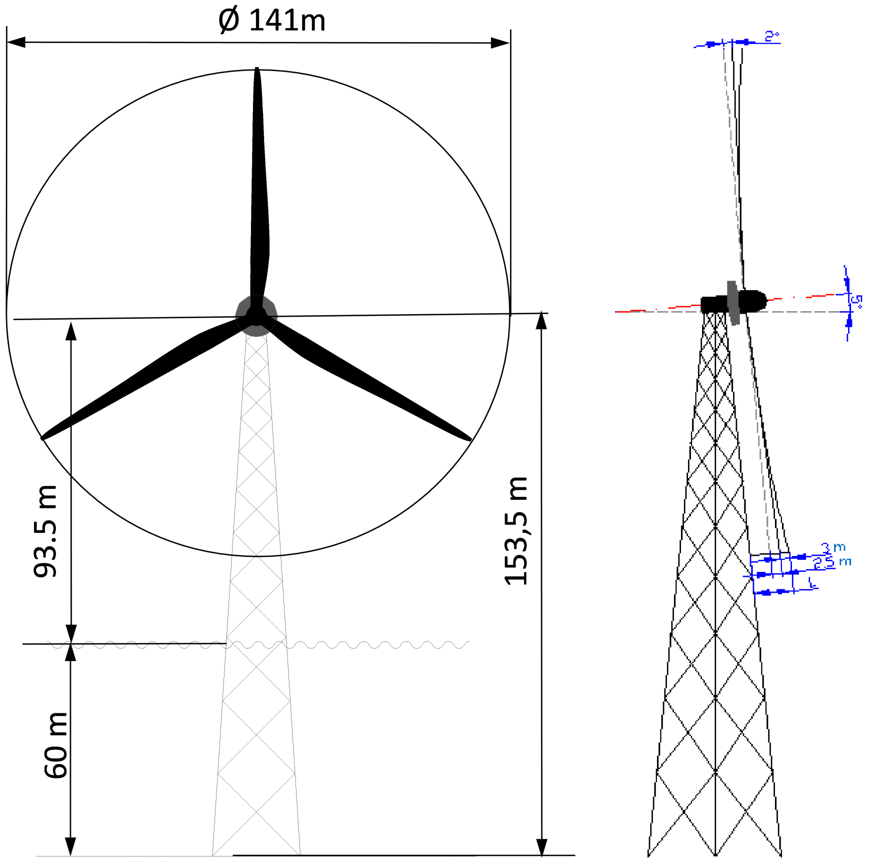

Figure 2: NOWITECH 10 MW reference turbine

2.1 Requirements

NOWITECH's design criteria are gathered in table 2.1. In addition to these requirements three parts of IEC 61400: Wind turbines, will be used:

- IEC 61400-1: Design requirements
- IEC 61400-3: Design requirements for offshore wind turbines
- IEC 61400-4: Design requirements for wind turbine gearboxes

For fatigue calculations, EN 13445-6 : Requirements for the design and fabrication of pressure vessels and pressure parts constructed from spheroidal graphite cast iron is used.

For the FLS analysis the hub, main shaft and bed plate have to withstand various loading through a lifetime of 20 years.

2.2 Previous work

Several thesis and PhDs have been written for the NOWITECH reference turbine. The relevant previous work for this thesis are:

Hub:	Mohammad Akram Khan[6] and Ebbe Berge Smith[7]
Main shaft:	Akram Khan[6] and Sandeep Singh Klair[7]
Bedplate:	Berge Smith[7] and Singh Klair[8]
Yaw Bearing:	Singh Klair[8]
Tower:	Ongoing PhD by Daniel Zwick

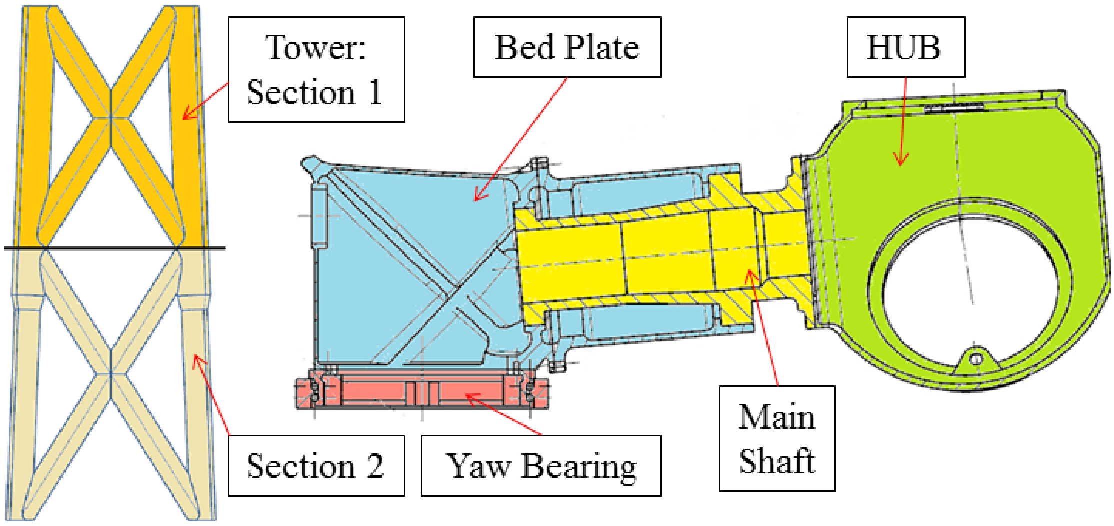

Figure 3: Top sections of tower and Yaw bearing, bed plate, main shaft, and hub

Table 1: Criteria for the NOWITECH turbine

	Symbol		Unit
Extreme wave height		30	m
Maximum sea current velocity		1.2	m/s
Water depth		60	m
Rated power output	P	10	MW
Electrical Frequency	fn	50	Hz
Weibull parameter	A	11.75	-
Weibull parameter	k	2.04	-
Density of air	ρ_{air}	1.225	kg/m^3
Density of seawater	ρ_{sea}	1025	kg/m^3
Water salinity		3.5	%
Water temperature (min/max)		0 / 22	$°C$
IEC turbulence parameter	I_{ref}	0.12	-
IEC reference wind speed	U_{ref}	50	m/s
Average wind speed at hub height	U_{ave}	10.4	m/s
IEC wind shear exponent	α	0.14	
Rotor diameter	D	141	m
Number of blades		3	-
Hub diameter	D_{Hub}	4.94	m
Length between blade tip and the tower	L	13	m
Maximum rotor speed	n	13.54	rpm
Maximum allowed tip speed		100	m/s
Extreme wind speed, 50 years	U_{e50}	70	m/s
Extreme wind speed, 1 year	U_{e1}	56	m/s
Design wind speed	$U_{Desgign}$	13	m/s
Rated wind speed	U_{Rated}	$\tilde{1}5$	m/s
Cut-in wind speed	U_{cut-in}	4	m/s
Cut-out wind speed	$U_{cut-out}$	30	m/s
Optimum tip speed ratio	TSR_{Opt}	7.8	-
Blade pre-curvature		3.06	m
Turbine blade coning angle		2	degrees
Main shaft tilt angle		5	degrees
Rotor weight (Generator)	G_{rotor}	60 000	kg
Stator weight(Generator)	G_{stator}	200 000	kg

3 Theory

3.1 Fatigue

When components are exposed to dynamic loading, fatigue failure can occur. Even if a part is going through stresses way below yield stress, it can lead to failure if the stresses are cyclic and repeated several times. Fatigue is caused by plastic deformation in microscopic scale. This would lead to a microscopic crack that could grow to a visible crack which again could cause failure. [9]

The SN-curve for a material could tell us how many times you could repeat a stress cycle ($\Delta\sigma$) before failure occurs (also called number of cycles, N). The SN-curve has a tendency to flatten out after a certain number of cycles, which means that if you expose a component to stresses under this limit, you get almost infinite number of cycles before failure. This stress limit is called the fatigue limit, σ_w.

3.1.1 Reduction Factors

The SN-curve is based on testing of cylindrical smooth specimens. In order to get good results for complex components in different environments and with various defects, we need to reduce the curve with different reduction factors or safety factors.

According to IEC 61400-4 the following reduction factors has an influence on the fatigue strength and shall be considered in calculation of the stress range:

- Partial factor for material, γ_m
- Partial factor for the consequence of failure, γ_n
- Surface roughness, f_s
- Wall thickness, f_e
- Temperature, f_t
- Mean stress, f_m
- Stress gradient
- Surface Treatment

NOTE: Partial factor for the consequence of failure are removed from the loads. The stress gradient and surface treatment are beneficial factors (not reduction factors) and are not considered in this thesis (conservative approximation).

3.1.2 Palmgren-Miner Rule

For variable amplitude loading Palmgren-Miner rule can be used to summarize the damage of each amplitude interval. By dividing the number of cycles the component is exposed for a certain amplitude loading with the number of cycles before failure with this load you get a damage factor. The Palmgren Miner rule says that when the sum of the damage factors for all the amplitude loads reaches 1, the life of the component is exhausted. [10]

$$\frac{n_1}{N_1} + \frac{n_2}{N_2} + \frac{n_3}{N_3} + ... = \Sigma \frac{n_i}{N_i} = 1 \tag{1}$$

3.2 Loads

Wind can cause many different load conditions on a wind turbine because of it is unpredictability. The wind varies in direction, strength and form (turbulence) and these loads are acting on the rotor blades. Other downstream components are also exposed to wind but compared to the force acting on the blades these are negligible.

In addition to wind loads, gravity, waves and loads from operating the wind turbine also have to be considered, see figure 4. [11]

The complexity of the wind crates several load cases that have to be considered. IEC 61400-1 presents design load cases (DLC) divided in different situations and wind conditions. For the ULS analysis of the transition piece DLC 1.3 is used. This is the load case where the highest stresses occur. [7] DLC 1.3 is simulating power production with a 50 year extreme turbulence model (ETM) for the wind condition [12]. This involves wind speeds between 4-30 m/s (see table 2.1).

Forces and moments presented in figure 5 are results from calculations done by Lars Frøyd in the aeroelastic software FAST. [12] The reference coordinate system for the loads is shown in figure 6.

According to IEC 61400-1 there are 5 design load cases that has to be considered for fatigue design: DLC 1.2(power production), 2.4 (failure), 3.1 (start up), 4.1 (normal shut down) and 6.4 (parked).

In this thesis only DLC 1.2 and 1.3 will be considered in the fatigue analysis. This are the only established fatigue loads NOWITECH have at the moment and it is also the most critical DLC for fatigue design (highest number of cycles). The DLC 1.2 and 1.3 are plotted in appendix A and illustrated in tables in chapter 17. DLC

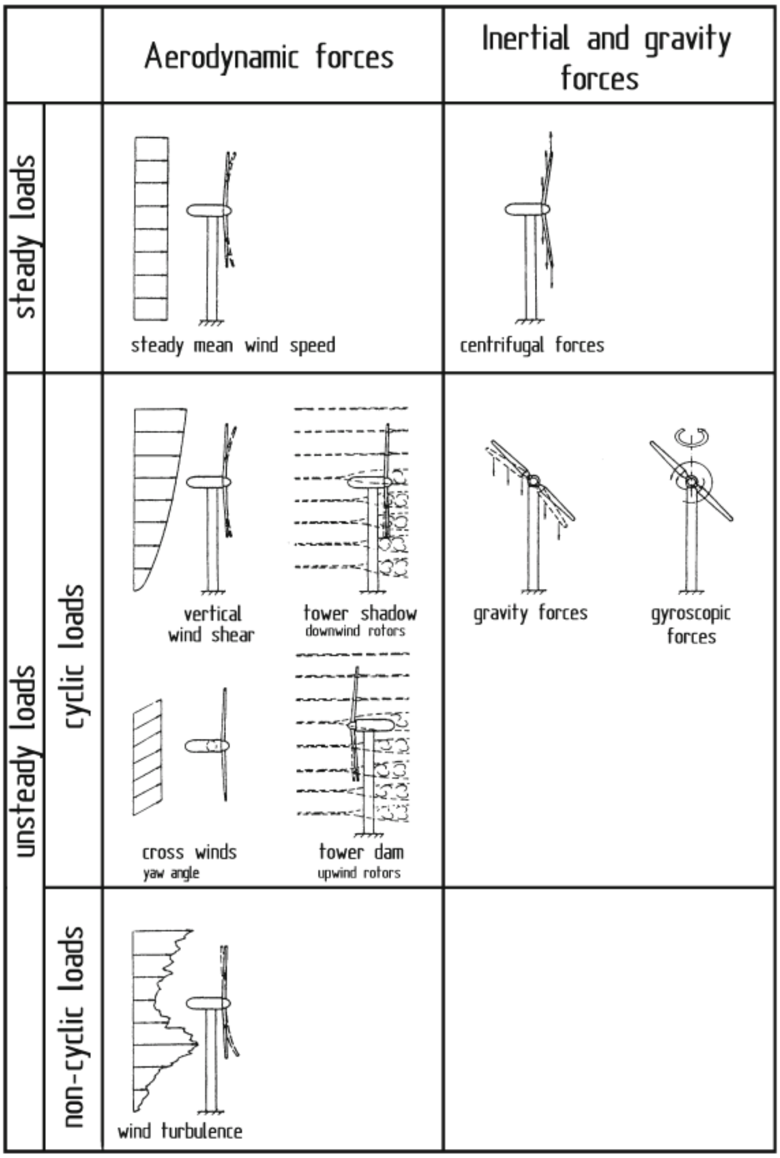

Figure 4: Forces acting on rotor [3]

1.2 has normal turbulence model and DLC 1.3 has extreme turbulence model. As mentioned only DLC 1.2 have to be considered in fatigue calculations according to IEC 61400-1, but the NOWITECH turbine is designed for wind farms where turbulence appear between the turbines. Therefore DLC 1.3 will be used for the FLS analysis instead of DLC 1.2.

1.3- Extreme Turbulence Model	Wind speed = 13m/s	Fx [kN]	1746	
		Fy [kN]	132	
		Fz [kN]	-1410	-1806
		Mx [kNm]	9129	
		My [kNm]	14550	-10440
		Mz [kNm]	15330	
	Ultimate loads	Fx [kN]	2176	
		Fy [kN]	340	
		Fz [kN]	-1542	-1919
		Mx [kNm]	11690	
		My [kNm]	28660	-16050
		Mz [kNm]	22480	

Figure 5: Loads in Design Load Case 1.3

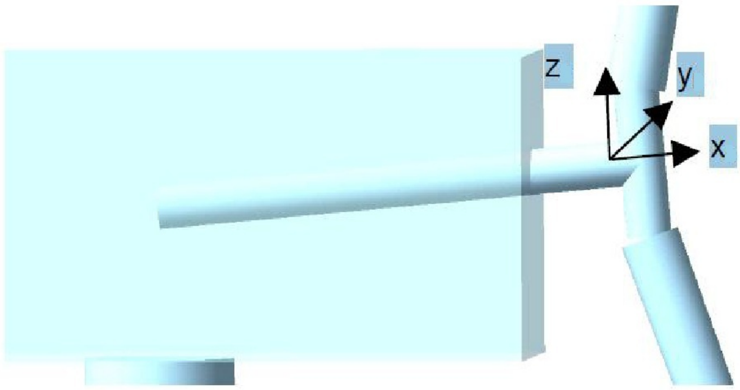

Figure 6: Reference coordinate system for loads

3.3 ULS Safety Factors

The ultimate limit state safety factors will be based on the DNV-DS-J102 standard [13]. It says that the characteristic load effects (S_d) from the FE-analysis, have to be compared with characteristic resistance (R_k). For this comparison there are several safety factors that have to be considered:

$$S_d(\gamma_f F_k) \leq \frac{R_k}{\gamma_m \gamma_n} \tag{2}$$

Where:

S_d	$=$	Load effect
γ_f	$=$	Load factor
γ_n	$=$	Consequence of failure factor
γ_m	$=$	Material safety factor
F_k	$=$	Characteristic load, see figure 5
R_k	$=$	Characteristic resistance, yield strength (R_m)

The load factor, $\gamma_f = 1.35$ for normal (N) load cases according to IEC [11] and the consequence of failure factor, $\gamma_n = 1.0$ for components that would lead to failure of a major part in the wind turbine. The material factor, $\gamma_m = 1.1$ for characteristic loads (F_k) equal to yield stress (R_p) and $\gamma_m = 1.3$ when F_k equals the tensile stress, R_m. Then the stress requirement for the ULS analysis has to follow:

$$S_d(1.35F_k) \leq \frac{R_k}{1.1 \cdot 1.0} \tag{3}$$

Part I

Transition Piece Design

4 Design Requirements

The transition piece needs to transfer all the loads from the yaw bearing to the tower according to the requirements explained in chapter 2.1. The yaw bearing cannot handle much deformation so the connection between the transition piece and the bearing requires enough stiffness. According to guidelines from NOWITECH th maximum weight is 50 tonnes per part in the top of the wind turbine (nacelle area).

In order to fit with the yaw bearing and tower, dimensions have to be gathered from Sandeep Sing Klair's model [8] and Daniel Zwick's model.

5 Concept 1

The first concept started with a simple ring with an outer diameter equal to the yaw bearing and a plate with dimensions as the top of the tower. A flange for bolt connection between the transition piece and the yaw bearing was designed. Then stiffeners was added in each corner to distribute the loads to the tower legs, see figure 7.

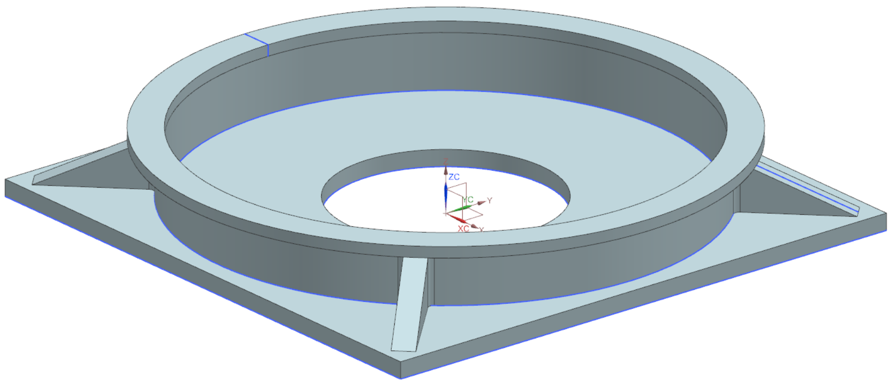

Figure 7: One of the first models

5.1 Optimization

In order to reduce the deformations in the flange the tube was extruded through the plate with 450 mm for increased stiffness. The stiffeners in each corner were increased to the edge of the flange to reduce stress concentrations between the stiffener and the flange. Edge blends in almost every corner and edge was also done for less stress concentrations. In the center a hole for maintenance access was created and later increased because the material had little impact on the stiffness and the increased hole contributes to weight reduction.

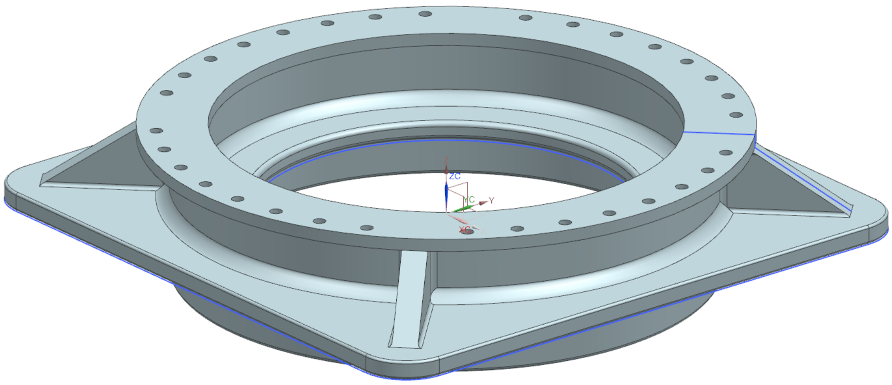

Figure 8: Optimization, concept 1

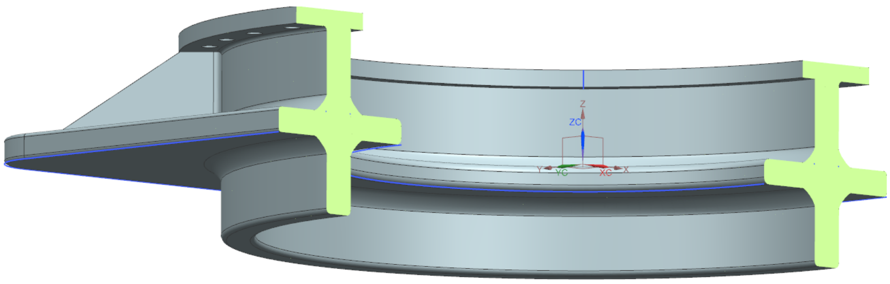

Figure 9: Section view, concept 1

5.2 Final Design

The final design consist of a flange with 36 (not 32 as in the previous design), 100 mm bolt holes for connection to the yaw bearing. This may be a bit conservative and have to be further discussed, however with 36 bolts the holes will not conflict with the stiffeners. The flange is extended towards center to minimize ovalization of the flange and increased stiffness in the bolt connection area. The outer diameter is 4740 mm, the same dimension as the outer diameter in the yaw bearing.

After a couple of simulations it was decided that the final design should have two stiffeners in each corner for better distribution of the loads to the tower legs. This caused the even placement of the 36 bolt holes. The stiffeners are placed to transfer loads on the tube/ring in each tower leg and not in the center as the previous stiffener.

The vertical pipe has a thickness of 200 mm, and is the thickest part of the component. Further increased thickness may result in higher strength but it also increase the probability of defects because of thicker cast iron. The total weight of this concept is 50.2 tonnes.

Despite the optimization of the design, the simulations revealed high stress concentrations in the 8 stiffeners and towards the center in each tower leg, see appendix D.

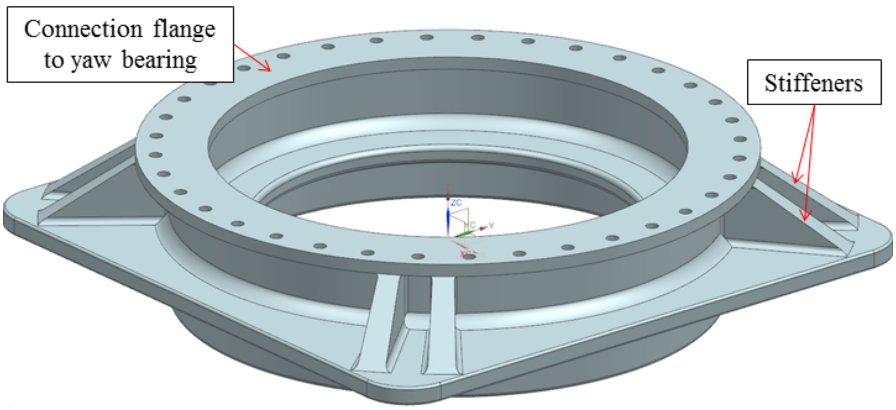

Figure 10: Final design

6 Concept 2

6.1 Tall Cone

Because of problems with stress concentrations in concept 1, a completely different concept was developed. The focus was to distribute the loads to the whole section of each tower leg since concept 1 had problems with that. It was also preferred to do this as organic as possible without sharp bends or corners.

In order to manage that, the height of the transition piece has to be increased. Since the height of the wind turbine is set according to design parameters in figure 2 (Hub height of 153.5 m), it was assumed that the tower had to be lowered. To do this without total redesign of the tower it was decided that the transition piece could replace the highest truss section of the tower (section 1 in figure 3).

The first concept 2 design is a main cone with top diameter equal to the inner diameter of the outer bearing ring and bottom diameter through the center of the tower legs. The main cone was first cut parallel to each side of the tower, but later moved further towards the center so the arc between each leg ended around the top of each tower leg. In each corner a smaller cone with dimensions according to each tower leg is blended into the main cone. The sharp edges were replaced with round curves and smooth edge blends. This design for replacement of tower section 1, placed on section 2 is called the tall cone.

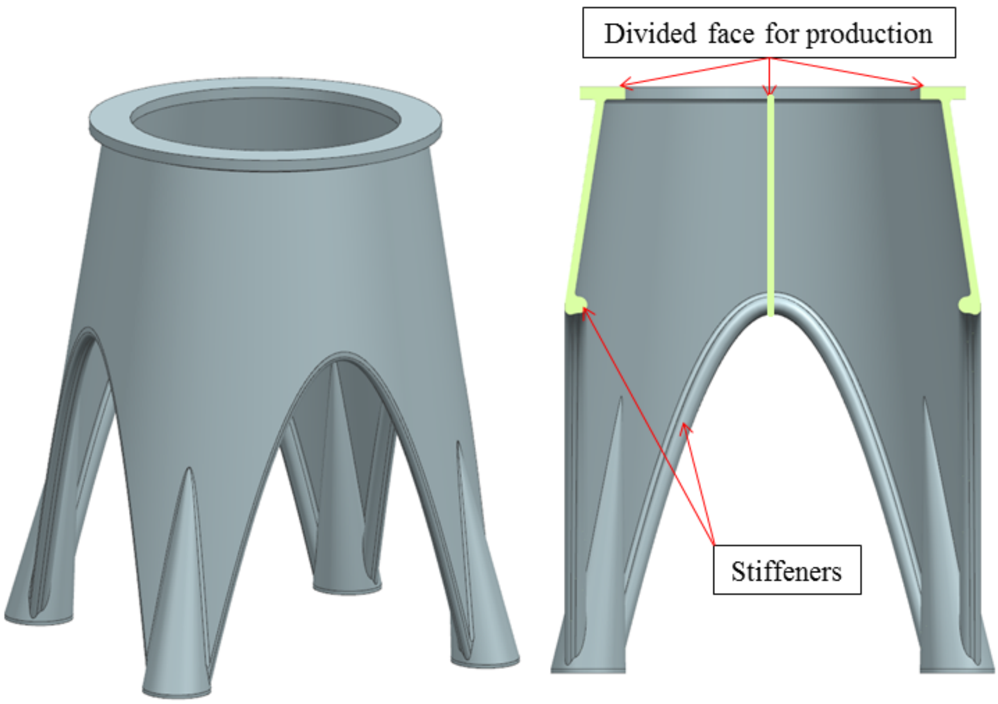

Figure 11: Concept 2, tall cone

Inside the tall cone a stiffener with radius 100 mm were added in the arc between each of the small cones to reduce stress problems in the curves between the feet. The thickness of the main cone was optimized to 100 mm after several simulations.

The total weight of this component is 82.5 tonnes which is rather good compared to concept 1 where the transition piece together with the top truss section of the tower have a total weight of:

$$m_{tot1} = m_{tower1} + m_{concept1} = 81.2\text{tonnes} + 50.2\text{tonnes} = 131.4\text{tonnes}$$

$$m_{tot2} = m_{concept2} = 82.5\text{tonnes}$$

The size creates problems when it comes to production of the component, the height is 7.2 m. One solution is to split it into four parts with a vertical bolt connection between each part through the top of each arc. Then it would be four identical pieces and equal casting mold for the four parts.

6.2 Short Cone

Because of the size of the tall cone it was decided to test a smaller version of the same concept. The height was set to 3150 mm because a lower one will result in a sharper angle between the tower legs and the yaw bearing that could cause too high stresses. The other dimensions were scaled from the tall cone which resulted in a weight of 53.4 tonnes. This design involves redesign of the tower in order to keep the required height.

The loads acting on the transition piece will force the four legs outwards and cause stresses in the arcs of the transition piece and between the diagonal tubes in the tower. To cope with this loads, stiffener pipes for tensile stress was added between the legs in the tower. This also require redesign of the tower but it is considered as a small change.

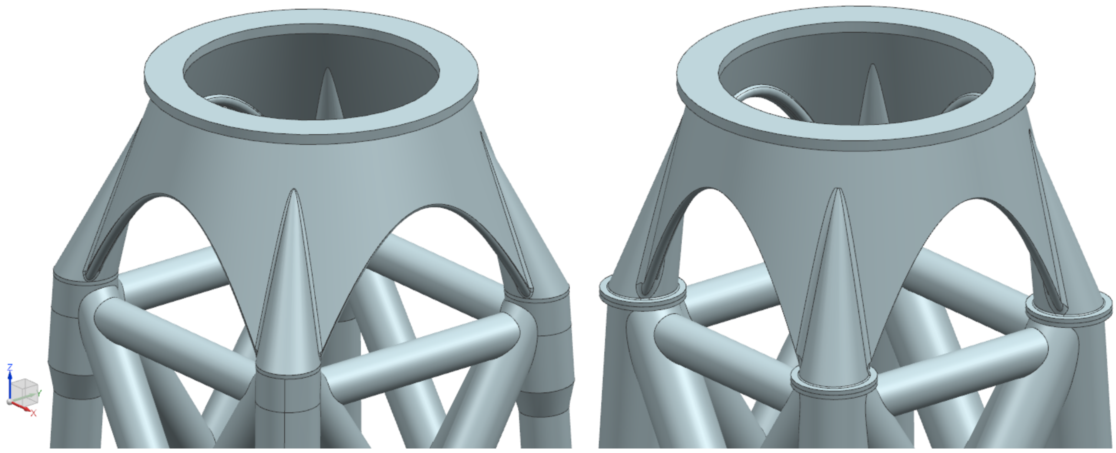

Figure 12: Short cone on tower section 2 (left) and section 1 (right)

6.3 Final Design - Short Cone

After a discussion with Karl Merz from NOWITECH it was decided that the total height of the reference turbine could be increased. Therefore the short cone could be placed on top of tower section 1. Then the angle in the transition piece would be smaller. The tower is also better suited for loading on the top section, because that section is reinforced with bigger dimensions (see figure 12 and 19).

Several simulations of the short cone had problems with stress concentrations in the connection area between the transition piece and the tower. To manage these stresses a flange for bolt connection was developed instead of welding directly to the tower.

There were also tried different edge blends in the area between the flange and where the arc ends. After some simulations it was founded that a combination of to different edge blends was the best alternative to reduce stress concentrations there. This combination was a 25 mm edge blend in the flange and a 80 mm edge blend (with a 250 mm center radius) in the end of the arc. To be able to cast the component with this flange, holes for casting was made. Two Ø200 mm holes in each leg for access to the hollow spaces (se figure 13). An alternative is to weld the plate with the holes, to the transition piece after casting. If the casting process, with the plate could be difficult. The mass of this final design is 49.6 tonnes.

7 Material Properties

Because of the complex structure, the transition piece is suggested to be made of cast iron. Material properties for the bed plate are not yet defined, but according to the design requirement for the bed plate of 200 MPa (max stress)[8], the material for the transition piece also have to handle that load in order to cast the parts in the same material. With this in mind a spheroidal graphite cast iron, EN-GJS-400-18 is suggested for the transition piece. This is a high strength ductile material defined in the material standard NS-EN 1563. EN-GJS-500-7 is also included in table 2, this is the alternative material with a higher yield and tensile strength.

The material data in table 2 and equation (2) in chapter 3.3, gives us the following requirement for maximum stress:

$$\frac{R_k}{\gamma_m \gamma_n} = \frac{240}{1.1 \cdot 1.0} = 218.2 \text{ MPa}$$

The alternative material, EN-GJS-500-7 has a yield stress of 290 MPa (see table

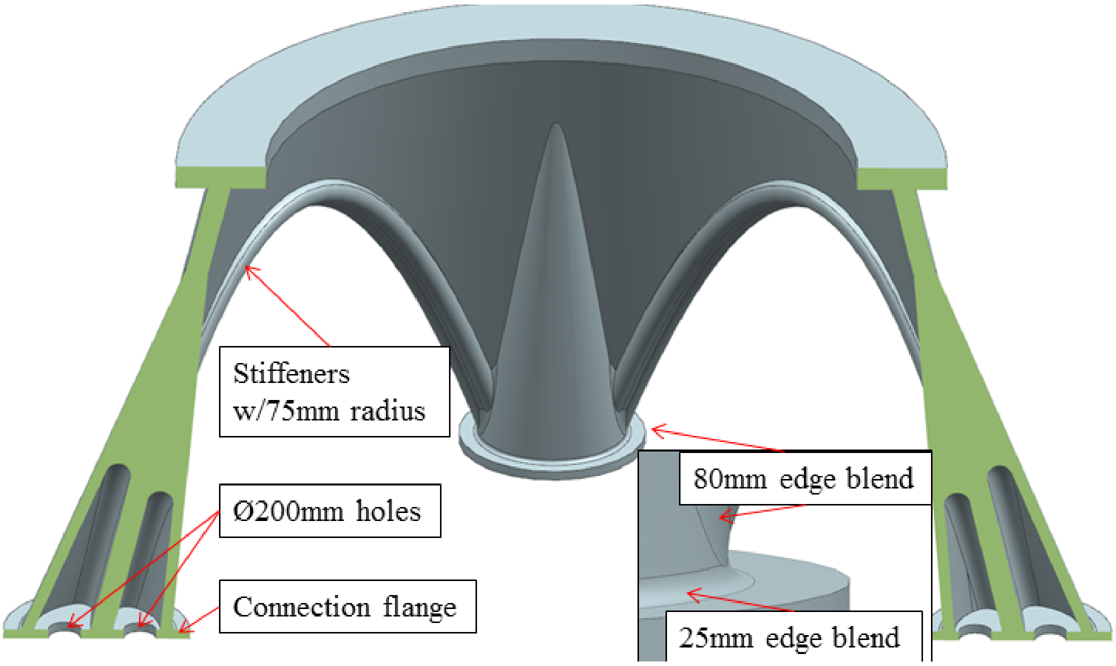

Figure 13: Section view of short cone with details

Table 2: Material data, transition piece

Material Designation	Youngs modulus, E [GPa]	Poissons ratio, ν	Density, $\rho[\frac{kg}{m^3}]$	Relevant thickness, t [mm]	Yield Strength, R_e [MPa]	Tensile strength, R_m [MPa]
EN-GJS-400-18	169	0.275	7100	$t \leq 30$ $30 > t \leq 60$ t > 60	250 250 240	400 390 370
EN-GJS-500-7	169	0.275	7100	t < 30 30 > t < 60 t > 60	320 300 290	500 450 420

2), this give us the following maximum calculated stress:

$$\frac{R_k}{\gamma_m \gamma_n} = \frac{290}{1.1 \cdot 1.0} = 263.6 \text{ MPa}$$

The price difference between the two materials is not known.

For the tower section a suitable material in NX was chosen, "Steel-Rolled" had a normal E-modulus and thus assumed to give good results with realistic deformations. The yaw bearing is made of high strength steel with high yield strength so the predefined material, AISI Steel 4340 was assumed to give good result with correct stiffness.

Table 3: Material data for yaw bearing and tower

Material Designation	Youngs modulus, E [GPa]	Poissons ratio, ν	Density, $\rho[\frac{kg}{m^3}]$	Yield Strength, R_e [MPa]	Tensile strength, R_m [MPa]
AISI_Steel_4340	193	0.284	7850	1178	1240
Steel Rolled	206	0.3	7850	235	340

8 Summary

Concept 1 is the smallest alternative, but not the lightest. It has sharp edges and corners and have problems with distribution of loads to the whole section of each tower leg. This component can be placed between the yaw bearing and the tower without changing the specified total height of the wind turbine. However there are still problems with high stresses that are difficult to reduce because of the design, see also appendix D.

Concept 2, the "cone" design is a more organic structure with less sharp edges and corners. It distribute the loads well to each legs cross section and it is higher/bigger than concept 1, but still not heavier in total. The first design (tall cone) could be placed on top of tower section 2 and do not require changed height of the wind turbine. It has a height of 7.2 m, something that could cause problems with handling, production and installing despite the suggestion of dividing the component into four identical sections.

The short cone has the same benefits as the tall cone but it is smaller and could therefore be produced in one piece. This design has sharper angle between the tower and yaw bearing than the tall cone design, this cause stress problems in each tower leg of section 2. However if the short cone is placed on top of tower section 1 the angle is reduced and so is the stresses. This requires reinforcement of the tower by adding tubes between each tower leg and also increased total height of the wind turbine.

9 FE Model

In order to create a realistic analysis for the transition piece, the model from Sandeep Sing Klair's thesis is used [8]. Combining it with the top part of the tower that Daniel Zwick has designed, see figure 3.

Only the FE model and simulations for concept 2, the short cone will be presented in this report. Most of the FE model presented here, are the same in the other simulations. Also some other results from the other designs are included in the appendix C and D.

9.1 Bed Plate

The bed plate designed by Singh Klair [8] was put in to the model but was reduced by taking off the nose part. The purpose of this was to reduce the simulation time. The bed plate, tower part was only included to add correct stiffness to the transition piece and will not be included in the results.

All components was meshed with 3D CTETRA(10) elements and for the bed plate a suggested average mesh size from NX of 197 mm was used.

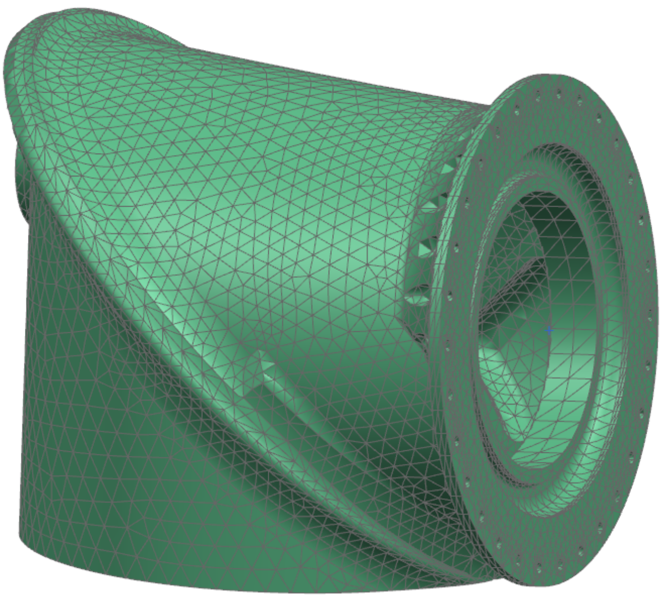

Figure 14: Meshed bed plate without nose part

In order to set the loads in center of the flange on the nose part there had to be created a RBE3 1D element with a spider node in center with node legs connected to all the nodes in the flange connection area, see figure 15. RBE3 element property, mean that the spider legs between the node in center and those in the flange cannot deform independently, an RBE2 element on the other hand add infinite stiffness to the structure. Therefore RBE3 is better suited for distributing pure loads.

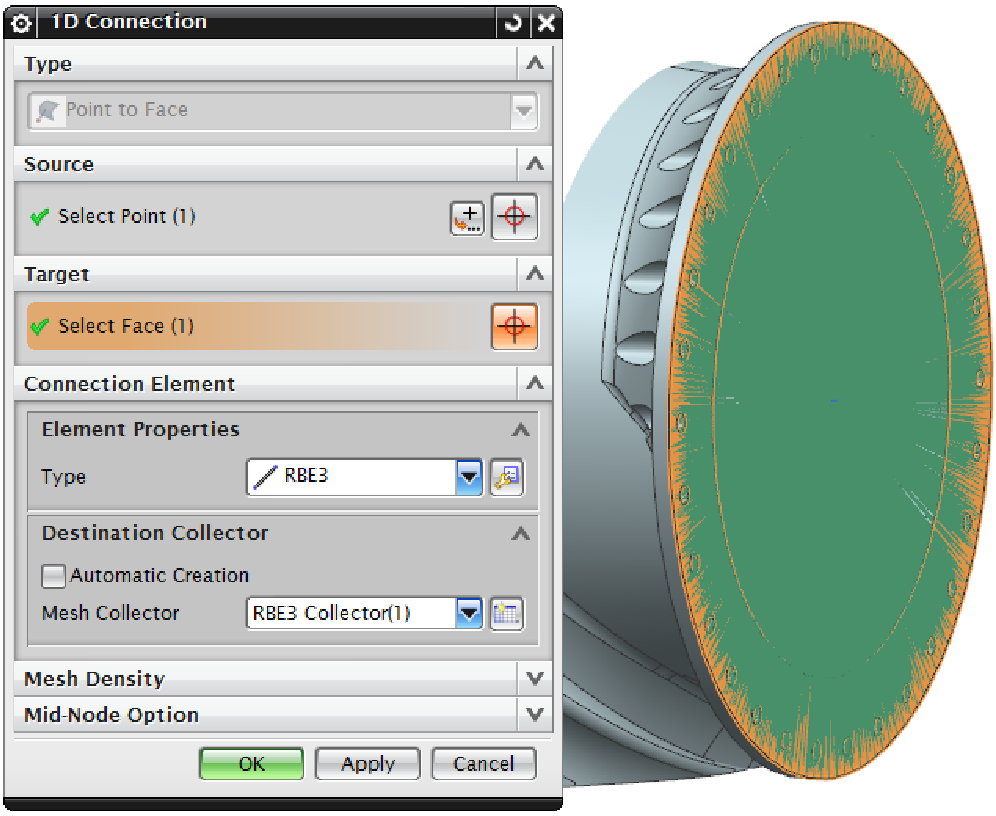

Figure 15: Spider connection on bed plate flange

9.2 Yaw Bearing

First the inner ring of the yaw bearing was changed because Sing Klair used "yaw locks" for locking the bearing since the transition piece was not designed. The yaw bearing will be operated by yaw motors and brakes attached to the inner and outer bearing ring. The section of the inner and outer bearing ring was changed so that the ball bearing rings would support the inner/outer bearing rings better.

The outer bearing ring is assumed to be bolted to the transition piece straight through the outer ring. In that way the outside face of the yaw bearing are free for mounting yaw motors. There are also room for placement of the motor and brakes inside the transition piece concept.

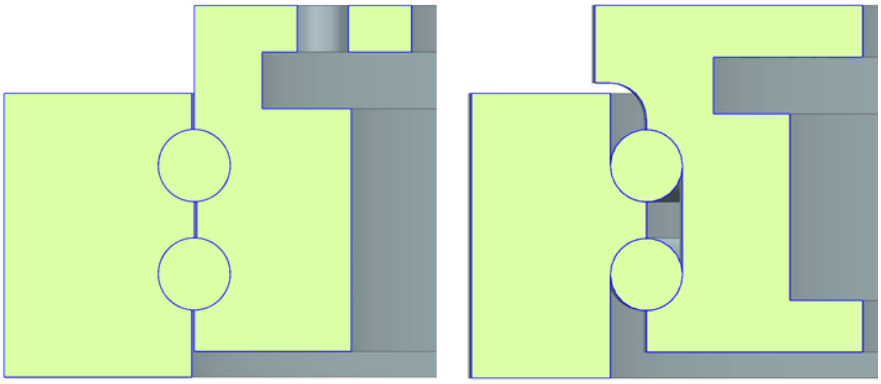

Figure 16: Section view of new (left) and previous (right) yaw bearing

It is difficult to get good results of ball bearings in non-linear FEM-analysis because of several assumptions taken like modeling of bearing rings instead of balls and other assumptions mentioned in chapter 11.2. There were several problems with simulation of the yaw bearing, this problems are also covered later in chapter 11.2.

The element sizes in the yaw bearing were set to 195 mm in the inner and outer bearing ring (same as bed plate). The bearing ring was meshed with 30 mm elements in order to get a realistic mesh. The contact surface against the inner and outer bearing rings was also set to 30 mm by "Mesh control" in NX. This resulted in a very long simulation time so the element sizes were increased to 50 mm.

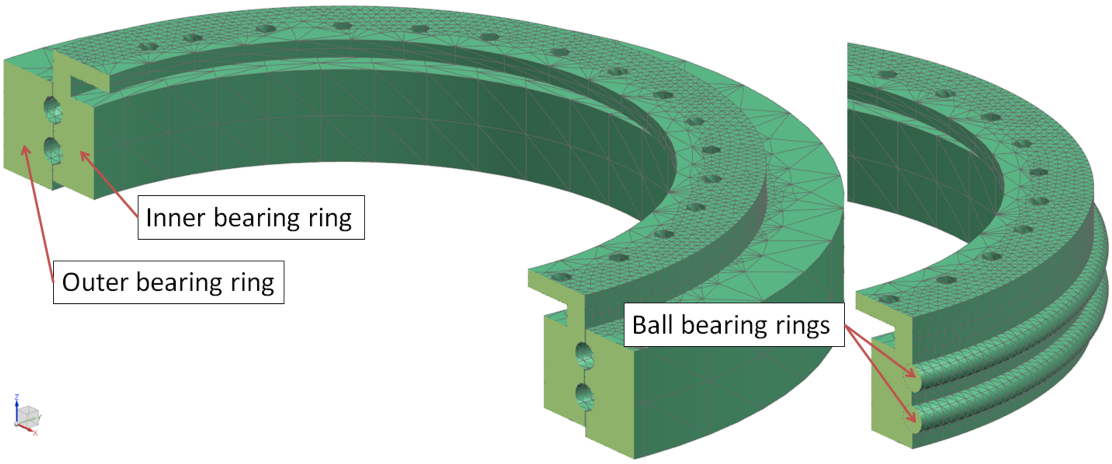

Figure 17: Meshed yaw bearing

NX are not suitable for dimensioning of ball bearings (see also chapter 11.2.2) and it was therefore included only to add correct stiffness to the transition piece.

9.3 Transition Piece

The short cone for tower section 1 were meshed with a suggested mesh size of 265 mm. Mesh control were used on several faces, in the arc between the legs and blends and transitions in the four legs see figure 18.

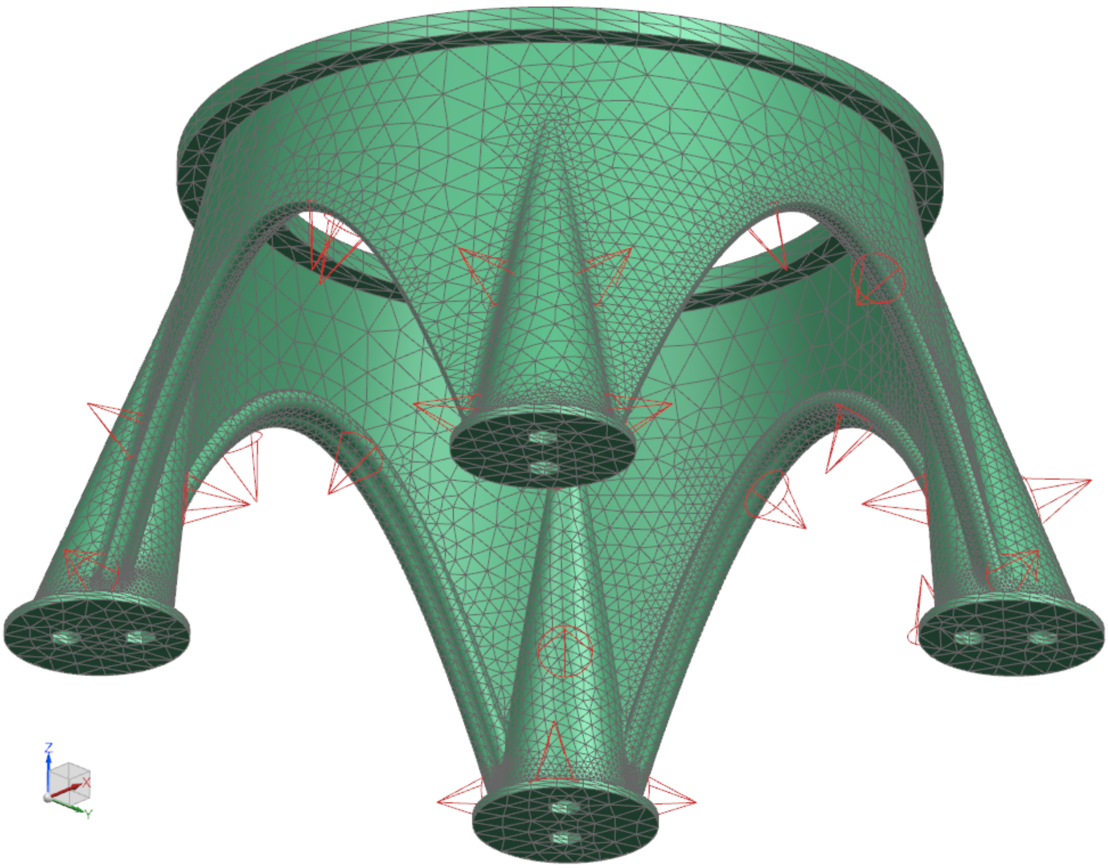

Figure 18: Mesh of the short cone with mesh refinement

9.4 Tower

As mentioned earlier there are used two different models of the tower. When analyzing concept 1 and the short cone in concept 2 the highest truss section of the tower (section 1) was used. In evaluation of the tall cone in concept 2 the second truss section (section 2) was applied to the model, see figure 19. The tower sections were added to the model in order to avoid artificial stiffness that a fixed constrain in the transition piece will do. The connection area between the tower and the transition piece could also be considered with reliable results.

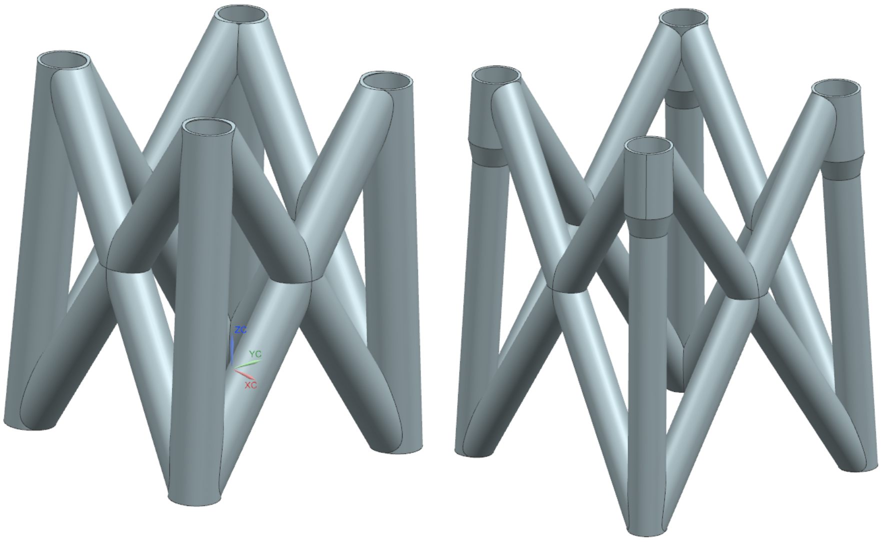

Figure 19: Tower section 1 (left) and section 2 (right)

Tower section 1 was meshed with 211 mm element size and this gives us the following table of all the mesh sizes used in the ULS simulation, (table 9.4):

Table 4: Mesh sizes for ULS analysis

Part	Mesh size [mm]
Bed plate, Tower part	195
Inner bearing ring	255
Ball bearing rings	50
Outer bearing rings	416
Transition piece	265
Tower section 1	211

10 Bolts

The contact surfaces in the bolt connections are glued instead of modeling bolts. First there were modeled, using 36 M100 bolts in the connection between the transition piece and yaw bearing. But after some simulations it was assumed that a glued contact surface would reduce the simulation time and also give better stress distributions. A detailed calculation of number of bolts and dimensions also has to be done to get better results. At the moment only rough estimations were found.

11 Simulation

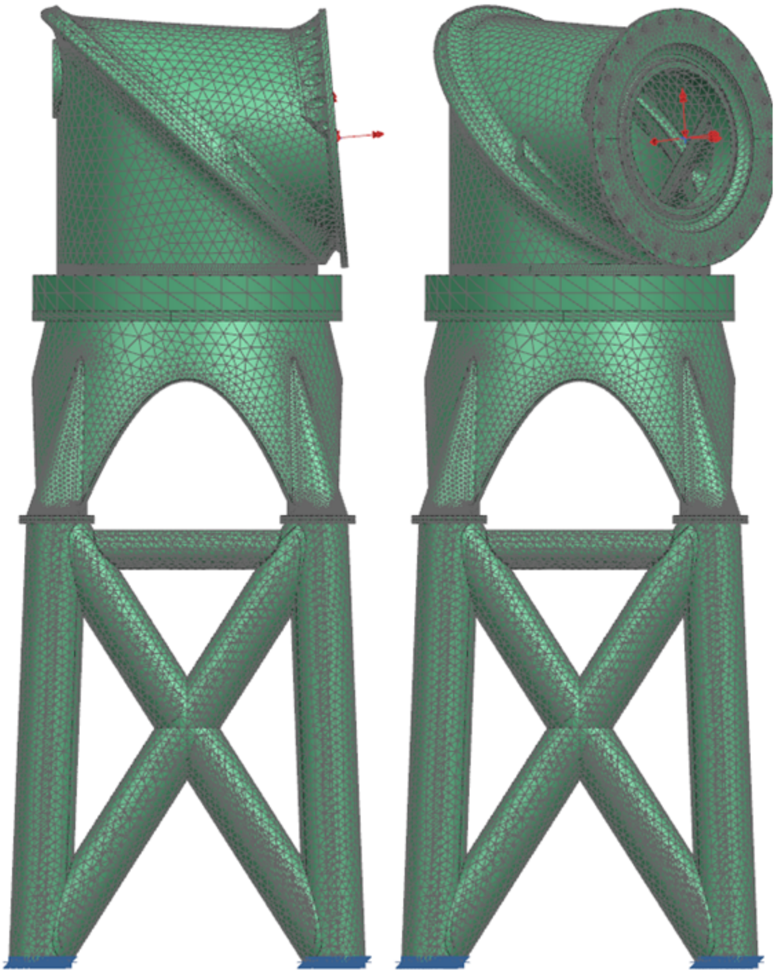

Figure 20: Complete model with load combination 1 and 2 shown

11.1 Loads

The loads given in figure 5 in chapter 3.2 are acting in the center of the rotor and hub (shown in figure 21). In order to apply the loads in the spider connection on the reduced bed plate (red cross in figure 21) instead of the center of the hub, they had to be converted. The converted loads are presented in table 5.

The weight of the generator, nose part of the bed plate, shaft and hub was added to the F_z load and this load together with the distances from the flange were again added to the M_y. In the same way F_y was added to M_z. Gravity was also added to the whole structure as a load in NX with acceleration of 9.81 m/s^2. There were also discovered that the direction of the F_x force had to be in the wrong direction, since the wind is pushing against the structure, not pulling. So the direction was changed and M_x was verified according to which way the rotor is turning (counter clockwise).

Table 5: Applied loads on bed plate

Load	Ref. Value	Contribute to	SF	Applied	Unit
F_x	2176	F_x	1.35	-2938	kN
F_y	340	F_y and M_z	1.35	459	kN
F_z	-1542	F_z and M_y	1.35	-6347	kN
M_x	11690	M_x	1.35	15781	kNm
M_y	28660	M_y	1.35	76729	kNm
M_z	22480	M_z	1.35	33899	kNm
$G_{generator}$	-2265	F_z and M_y	1		kN
$G_{structure}$	-2000	F_z and M_y	1		kN

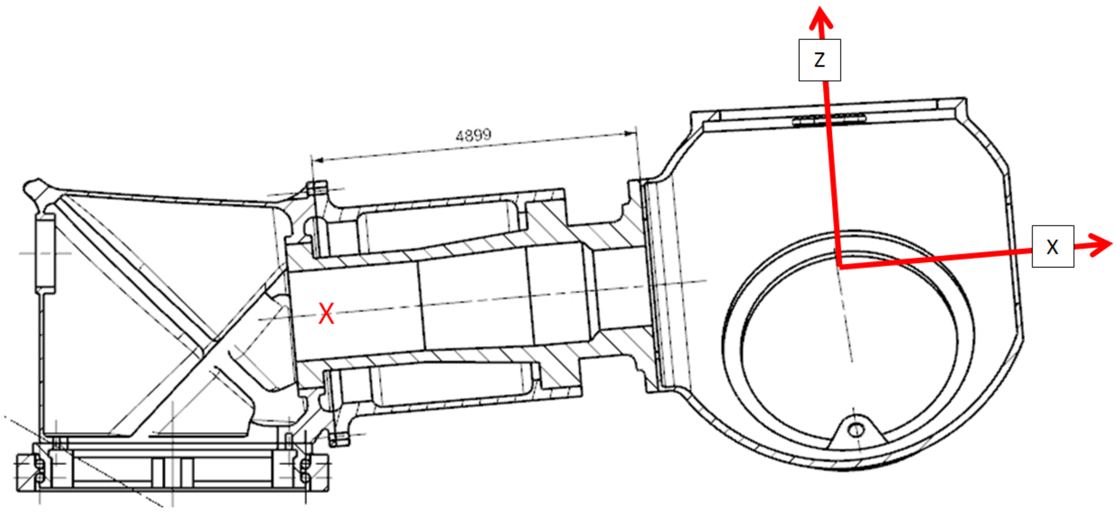

Figure 21: Converted coordinate system

Since the transition piece and tower are plane symmetrical and not axis symmetrical, a simulation with the nacelle 45 degrees on the tower also had to be performed. M_y and M_z direction can change as the wind direction change and therefore create four load combinations. From the sizes of the loads in table 5 we can assume that a positive M_y and M_z will be the most critical load combination because they are adding up F_z and F_y. This is also shown in Singh Klair's results [8]. So there are two load combination that would be tested, load combination 1: 0° and load combination 2: 45° (see figure 20).

11.2 Boundary Conditions

11.2.1 Fixed Constrains

Each face on the bottom of the four legs were constrained in all directions as shown in figure 22. A fixed constrain like this will add infinite stiffness in these surfaces, but will not affect the results in other parts of the model except from the bottom part of the tower section.

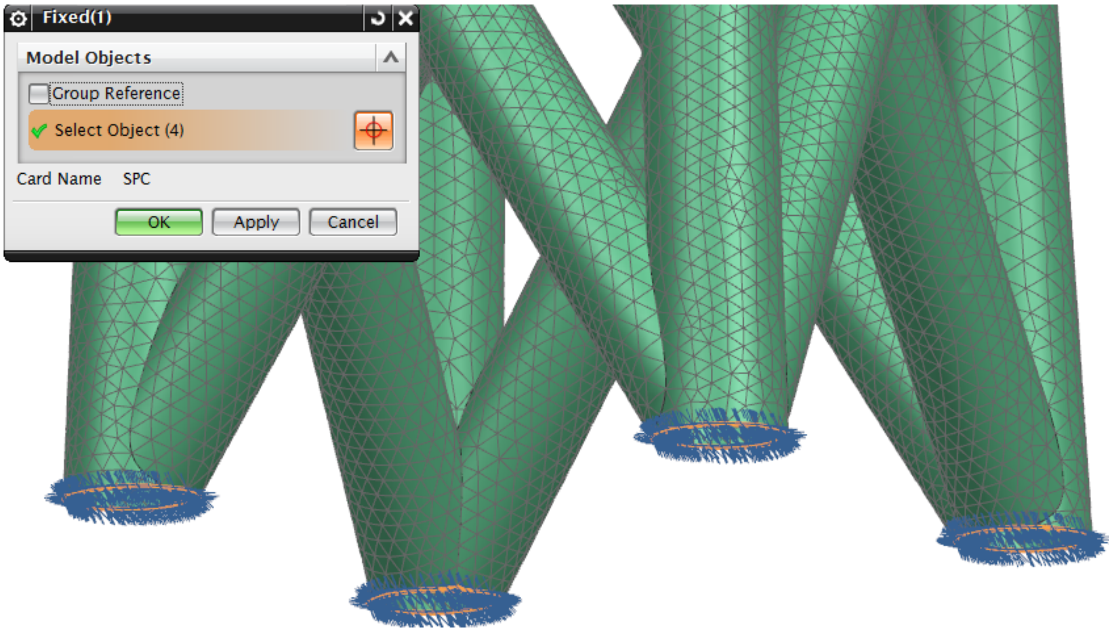

Figure 22: Fixed constraints

11.2.2 Contact Surfaces

First the yaw bearing was simulated with a combination of glued and sliding contact surfaces: The ball bearing rings were glued to the inner bearing ring using "surface-to-surface gluing" function in NX, and gliding contact against the outer bearing ring using "surface-to-surface contact".

With surface-to-surface gluing NX will merge the mesh between the components in the contact area. The stress distribution around the yaw bearing would be unrealistic because the bearing rings could handle tensile stress with glued contact. In reality they are only exposed for compression stress.

With the combination of glued and gliding contact the results reviled von-Mises stresses with values up to 40000 MPa, see appendix C. Therefore it was decided to set "surface-to-surface gluing" instead of "surface-to-surface contact" between the inner ring, bearings rings and outer bearing ring.

To verify this assumption a model of just the yaw bearing was build. Two simulations with a load of only 1 kN was completed, one with glued contact and another with the combination of glued and gliding contact. This revealed over 700 MPa stresses in the gliding contact surface and almost 0 MPa (0.09 MPa) in the same surface when glued contact was applied.

After gluing the yaw bearing together the simulation time was reduced to just 20 minutes, something that made it possible to run several simulations per day and do small detail changes between each simulation to optimize the design and model faster.

12 Results

12.1 Concept 2

12.1.1 Load Combination 1: 0°

DLC 1.3 - Extreme Turbulence Model, Load comb. 1: 0°		
Max. Von-Mises	Max. strain	Comments
252.6 MPa	0.00127 mm/mm	15 nodes with stresses above yield
Confidence level (mesh quality): 95.628%		

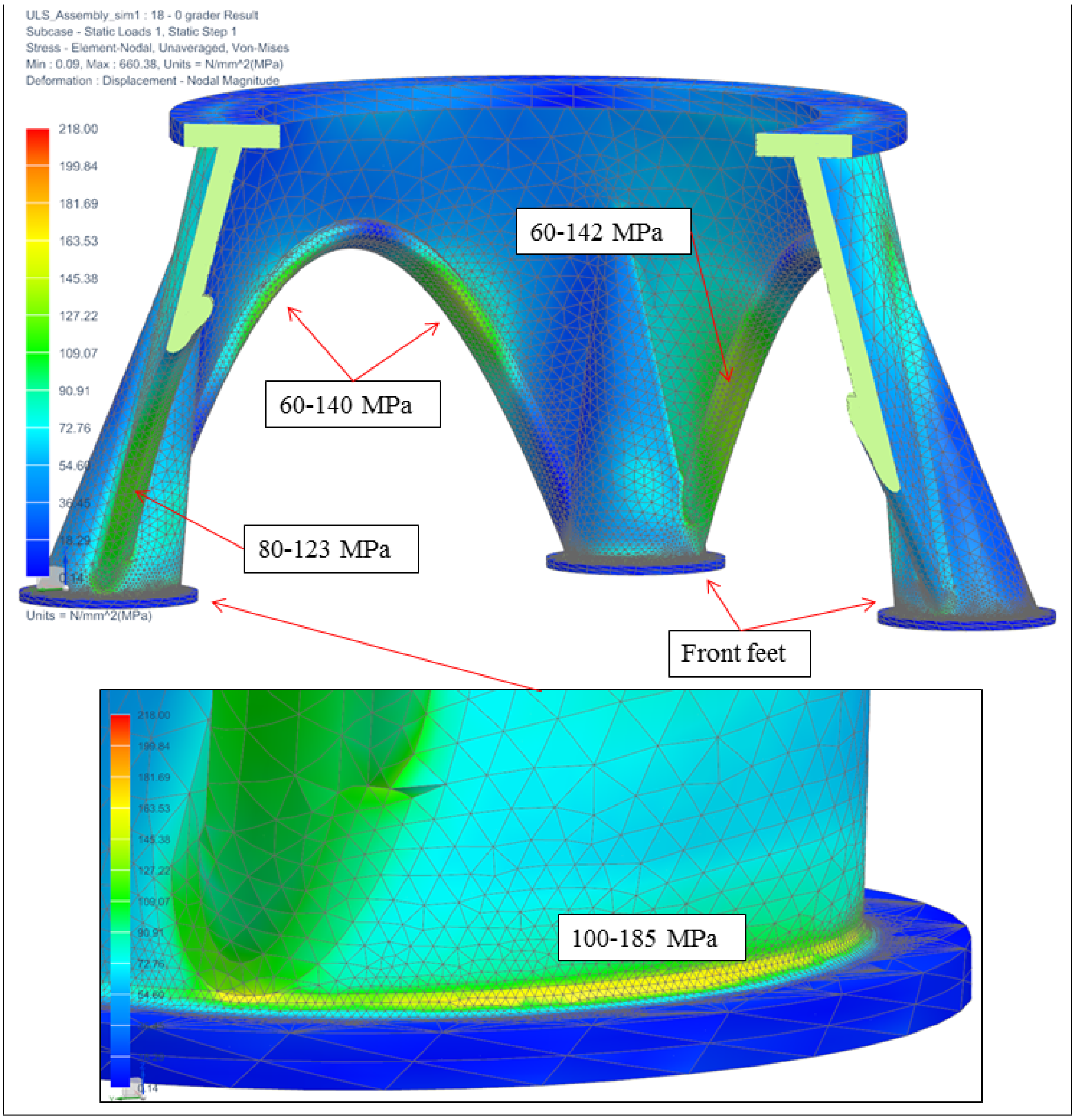

DLC 1.3 - Extreme Turbulence Model, Load comb. 1: 0°
Maximum Von Mises stress seen from the front

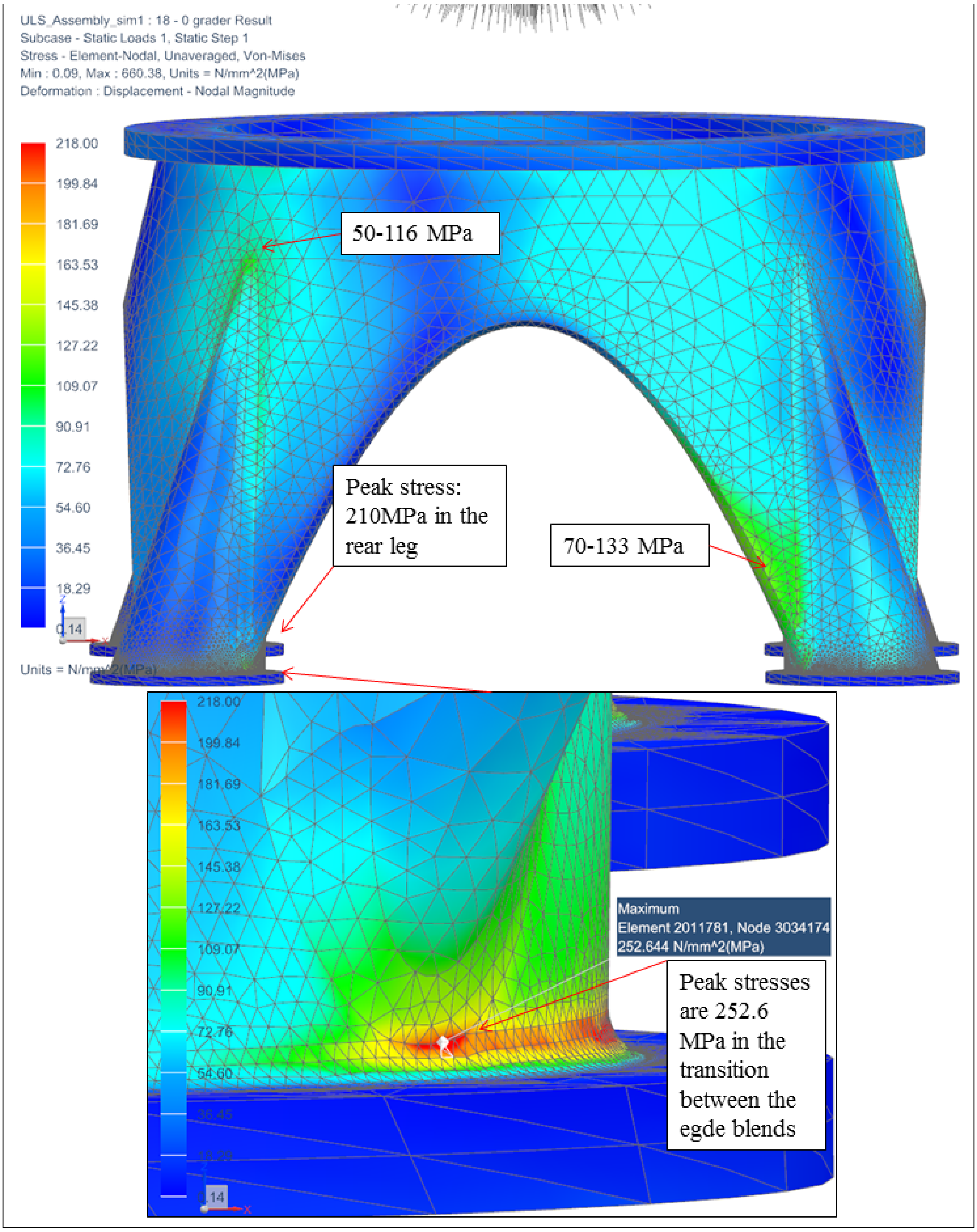

12.1.2 Load Combination 2: 45°

DLC 1.3 - Extreme Turbulence Model, Load comb. 2: 45°		
Max. Von-Mises	Max. strain	Comments
262 MPa	0.00132 mm/mm	48 nodes with stresses above yield
Confidence level (mesh quality): 95.645%		

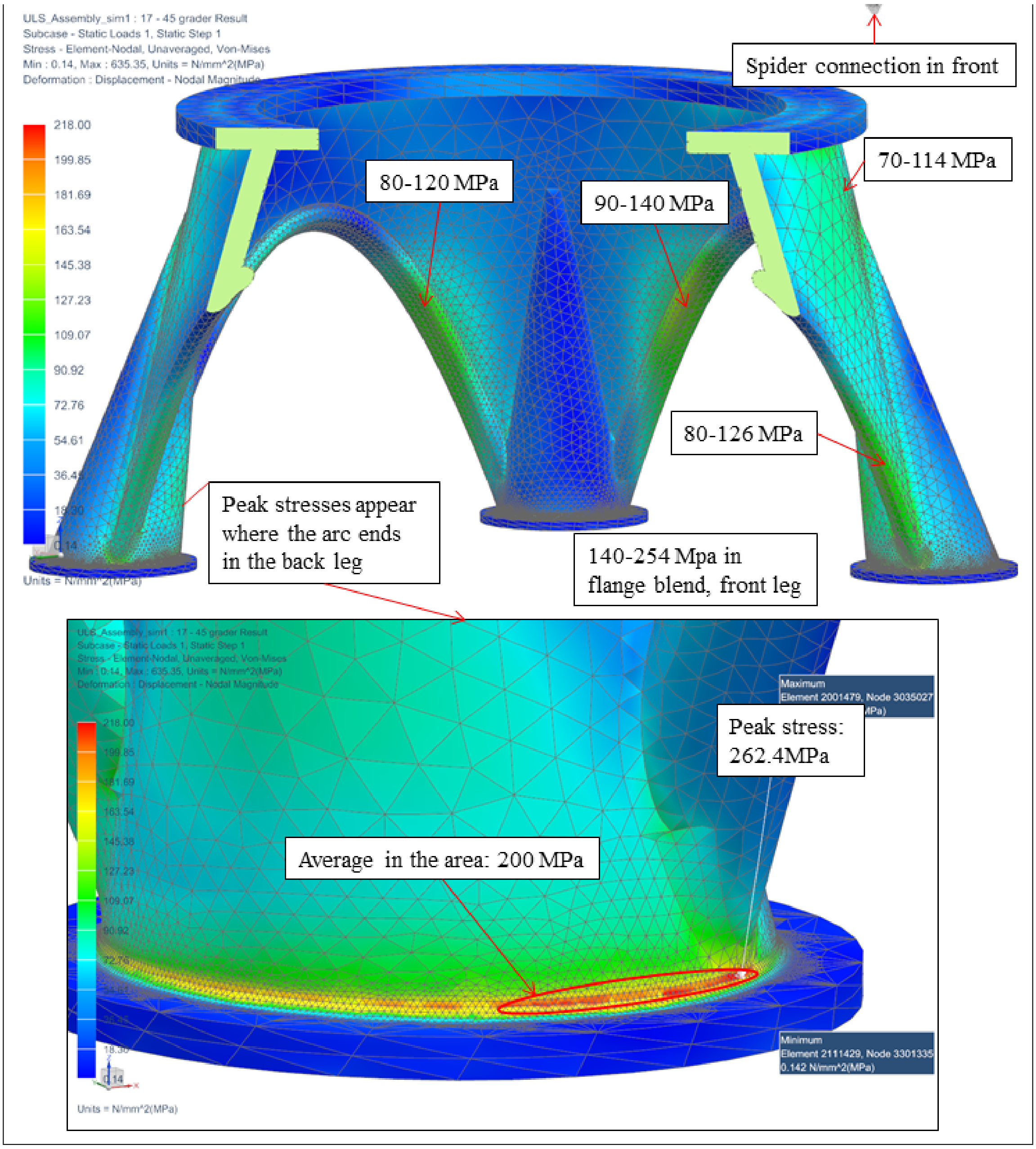

12.2 Displacement

Displacement in z-direction		
Load combination	Max	Min
1, 0 degrees	2.92 mm	-3.3 mm
2, 45 degrees	2.84 mm	-3.28 mm

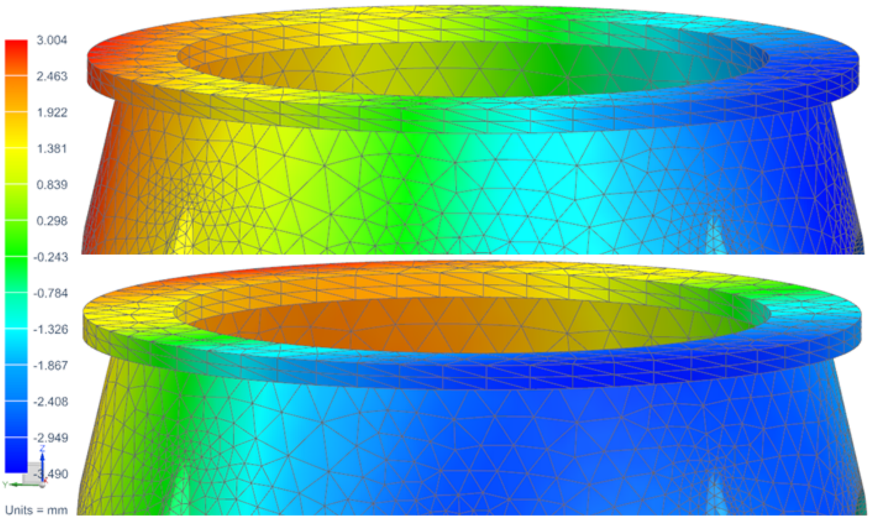

Figure 23: Displacement in z-direction, load comb. 1 above and 2 underneath

12.3 Discussion

Stresses in the transition piece will vary as the turbine is turned up against the wind.

In load combination 1 there are some critical areas (see chapter 12.1.1): The peak stress are located in the transition between the two edge blends where the arc between the front legs meet the connection flange. As mentioned in chapter 6.3, different edge blends was tried here. The peak stress of 252 MPa appear in one node, the neighboring nodes have values of 242, 222, and 221 MPa. The average von-Mises stress for the 24 neighbor nodes in the edge between the two edge blends are 223 MPa which could be a more reliable value. There are 15 nodes in the transition piece that have stresses above yield. These nodes are situated in the edge blend to the right of the maximum peak stress and the peak stress node.

The maximum stress in the other legs are also located in the root of the flange but a little distance from the arc as seen in chapter 12.1.1. They are also lower than in the right front (RF) feet, respectively 210, 185 and 157 in the right rear (RR), left rear (LR) and left front (LF). This is just below the allowable maximum stress limit of 218 MPa.

There are several other exposed areas in the transition piece for load combination 1, these are mainly in the arcs between the legs. The maximum stresses here do not exceed 142 MPa and are considered as reliable. This is mostly because the maximum stress is located in several elements, not in just a couple of nodes.

The DLC 1.3 and gravity loads are pushing the front of the transition piece down and therefore result in compression stress in the front of the transition piece and tensile stress at the back.

In load combination 2 the peak stress is higher (262 MPa) and located in the same edge but in the rear leg (on the opposite side of the rotor). This is 22 MPa above yield stress and 44 MPa above maximum allowable stress. But it is only 11 nodes with stresses above yield in the rear foot. In the front foot the maximum von-Mises stress is 254 MPa and there are 37 nodes above yield stress.

The confidence level for the two simulations were above 95% which mean that the mesh quality in the model is good and do not need further refinement.

The displacement of the connection flange for the yaw bearing in z-direction is shown in figure 23. The actual allowance of displacement is not known, but the displacements are plane and the maximum and minimum displacement are almost the same in both load combinations. This contributes to less wear of the bearing raceway. Seen from above there are some ovalization of the same flange, this could be improved by expanding the flange towards center for increased stiffness against ovalization.

Gluing of the yaw bearing may have resulted in incorrect stiffness in connection flange of the transition piece, see chapter 11.2.2 for further information. But all the stresses in the top part of the transition piece are way below the maximum stress requirement($<$ 115 MPa) and it is therefore believed that a more correct simulation of the yaw bearing would not cause critical stresses.

Part II

Fatigue Analysis

For the FLS analysis EN 13445-6 will be used, this standard specifies requirements for a simplified and a detailed assessment of fatigue life for spheroidal graphite cast iron. The guidelines for the detailed assessment will be used. To verify the lifetime of 20 years the damage factor from Miner's rule mentioned in chapter 3.1.2 will be used.

13 Material Properties

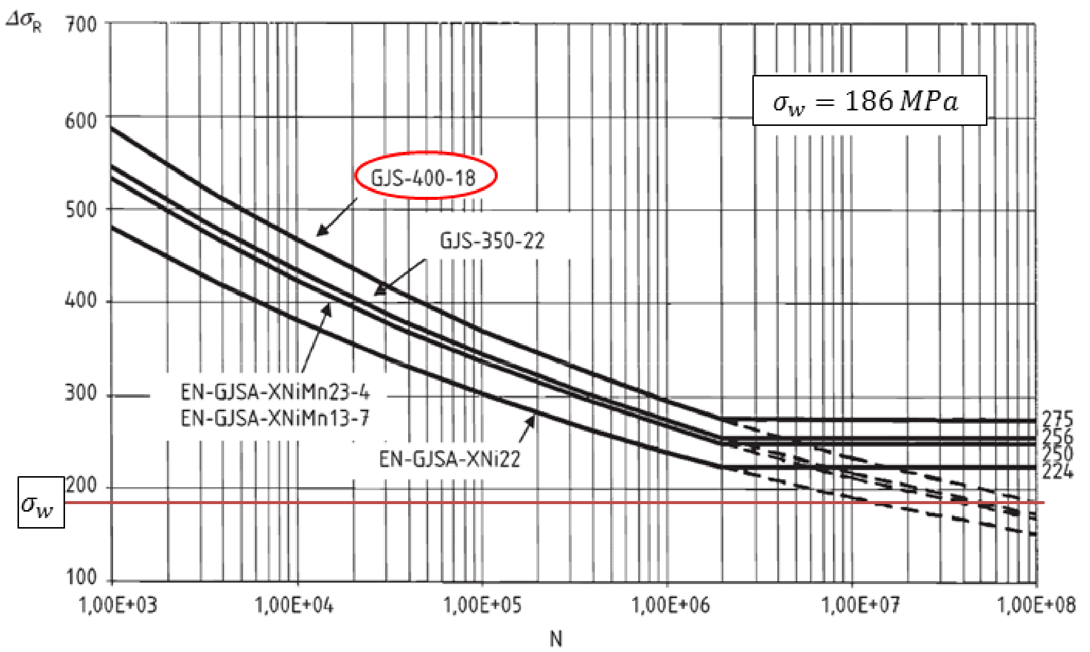

Figure D.2 — Fatigue design curves for ferritic and austenitic spheroidal graphite cast iron grades at ambient temperature - Detailed assessment

Figure 24: SN curve for detailed assessment from EN 13445-6

$$\Delta\sigma_R = 2\sigma_a = \frac{C_c}{N^{\frac{1}{m}}} = \frac{1173}{N^{0.1}} \tag{4}$$

for $10^3 < N < 10^8$

14 FLS Safety Factors

As mentioned in chapter 3.1.1, the following reduction factors have been calculated.

14.1 Partial Factor for Material

Since the test results for the material properties of EN-GJS-400-18, in NS-EN 1563 are developed with 97.7% survival probability the partial factor for material, γ_m is:

$$\boldsymbol{\gamma_m = 1.1}$$

for cast iron, according to IEC 61400-4.

14.2 Partial Factor for the Consequence of Failure

The partial factor for the consequence of failure, γ_n is given by IEC 61400-1 and is dependent on the component class. Since all parts in this FLS analysis are in class 2 ("non fail-safe" structural components whose failures may lead to the failure of a major part of a wind turbine),

$$\boldsymbol{\gamma_n = 1.1}$$

for all components.

14.3 Surface Roughness

The equation for calculating surface roughness, f_s are given in EN 13445-6:

$$f_s = F_s^{0.1ln(N)-0.465} \tag{5}$$

where N equals number of cycles and

$$F_s = 1 - 0.03 \cdot ln(R_z) \cdot ln(\frac{R_m}{200}) = 0.902 \tag{6}$$

R_z is a value who tells us the peak to valley height in μm for the surface finish. $R_z = 200\mu m$ (when R_z is unspecified) and $R_m = 370$ MPa (table 2)

Then the surface roughness reduction factor for each n value and for every component will be (see chapter 16.1 for explanation of the n-values):

Table 6: Surface roughness reduction factors

n, 1 year	n, 20 years	$\boldsymbol{f_s}$
$9 \cdot 10^2$	$1.8 \cdot 10^4$	**0.95**
$9 \cdot 10^3$	$1.8 \cdot 10^5$	**0.93**
$9 \cdot 10^4$	$1.8 \cdot 10^6$	**0.90**
$9 \cdot 10^5$	$1.8 \cdot 10^7$	**0.88**
$9 \cdot 10^6$	$1.8 \cdot 10^8$	**0.86**

14.4 Wall Thickness

Also in EN 13445-6, the equation for wall thickness,f_e is specified as:

$$f_e = F_e^{0.1ln(N)-0.465} \tag{7}$$

where

$$F_e = \left(\frac{25}{e_{max}}\right)^{0.182} \tag{8}$$

e_{max} is the maximum thickness for the component and for $e_{max} > 150mm$, the value of f_e for $e_{max} = 150$ mm applies. Then:

$$F_e = \left(\frac{25}{150}\right)^{0.182} = 0.722$$

for all parts since e_{max} is greater than 150 mm.

Thus give a set of wall thickness reduction factor for every component, see table 7.

Table 7: Wall thickness reduction factors

n, 1 year	n, 20 years	f_e
$9 \cdot 10^1$	$1.8 \cdot 10^3$	**0.91**
$9 \cdot 10^2$	$1.8 \cdot 10^4$	**0.85**
$9 \cdot 10^3$	$1.8 \cdot 10^5$	**0.78**
$9 \cdot 10^4$	$1.8 \cdot 10^6$	**0.73**
$9 \cdot 10^5$	$1.8 \cdot 10^7$	**0.73**
$9 \cdot 10^6$	$1.8 \cdot 10^8$	**0.67**

14.5 Temperature

For temperatures below 100 °C the temperature reduction factor is

$$\boldsymbol{f_t = 1}$$

for all components.

14.6 Mean Stress

According to EN 13445-6 the mean stress sensitivity factor for spheroidal graphite cast iron is:

$$M = 0.00035 \cdot R_m + 0.08 = 0.00035 \cdot 370 + 0.08 = 0.21$$

For purely plastic behavior the mean stress reduction factor, f_m is:

$$f_m = \left[1 - \frac{M(2+M)}{1+M}\left(\frac{2\bar{\sigma}_m}{\Delta\sigma_R}\right)\right]^{0.5} \quad , \text{for} \quad \sigma_m < \frac{\Delta\sigma_R}{2(1+M)} \tag{9}$$

and

$$f_m = \frac{1+\frac{M}{3}}{1+M} - \frac{M}{3}\left(\frac{2\bar{\sigma}_m}{\Delta\sigma_R}\right) \quad , \text{for} \quad \frac{\Delta\sigma_R}{2(1+M)} \leq \sigma_m \tag{10}$$

where $\Delta\sigma_R$ is the maximum equivalent stress range for a corresponding number of cycles(see the SN-curve, figure 24) and $\bar{\sigma}_m$ is the highest mean stress in each component:

Table 8: Highest mean stress

Component	$\bar{\sigma}_m$ [MPa]
Main shaft	12
Bed plate, NP	28
Bed plate, TP	52
Transition piece	90

The calculation of the highest mean stress is taken from the mean stress simulation. Since $\Delta\sigma_R$ is dependent of number of cycles applied, the reduction factor changes with n and will decrease as $\Delta\sigma_R$ decrease:

Table 9: Mean stress reduction factors

n, 20 years	Main Shaft $\boldsymbol{f_{m,MS}}$	Bed plate, NP $\boldsymbol{f_{m,BPNP}}$	Bed plate, TP $\boldsymbol{f_{m,BPTP}}$	Transition piece $\boldsymbol{f_{m,TP}}$
$1.8 \cdot 10^3$	0.99	0.98	0.96	0.94
$1.8 \cdot 10^4$	0.99	0.98	0.95	0.92
$1.8 \cdot 10^5$	0.99	0.97	0.94	0.90
$1.8 \cdot 10^6$	0.98	0.96	0.93	0.87
$1.8 \cdot 10^7$	0.98	0.95	0.91	0.83
$1.8 \cdot 10^8$	0.97	0.94	0.88	0.81

14.7 Overall Safety Factor

The overall safety factor i defined by the following

$$S_f = \frac{\gamma_m \gamma_n}{f_s f_e f_t f_m} \tag{11}$$

Since f_s and f_e are dependent on the number of life cycles, n these factors have to be calculated for each n.

Table 10: Total safety factors

n, 20 yr	Main Shaft S_f	Bed plate, NP S_f	Bed plate, TP S_f	Transition piece S_f
$1.8 \cdot 10^3$	1.44	1.46	1.49	1.53
$1.8 \cdot 10^4$	1.59	1.61	1.65	1.71
$1.8 \cdot 10^5$	1.77	1.81	1.86	1.95
$1.8 \cdot 10^6$	1.95	1.99	2.07	2.206
$1.8 \cdot 10^7$	2.00	2.07	2.17	2.36
$1.8 \cdot 10^8$	2.25	2.34	2.49	2.69

15 Allowable Number of Cycles

From the SN-curve we can find allowable number of cycles, N:

$$N = \left(\frac{C_c}{\Delta\sigma_R}\right)^m = \left(\frac{1173}{\Delta\sigma_R}\right)^{10}$$

where

$$\Delta\sigma_R = \frac{2\sigma_{eq}\gamma_m\gamma_n}{f_s f_e f_t f_m} = 2\sigma_{eq}S_f$$

and σ_{eq} is the stress amplitude calculated from the r-values in chapter 17 together with the FLS loads in chapter 16.1.

16 Simulation

Originally the simulation was supposed to be run in FEDEM 7.0 windpower using a dynamic simulation. Due to the increased work with designing the transition piece, and poor knowledge of FEDEM it was decided to do the simulation in NX/Nastran instead. This may give less accurate results and therefore compensated by more conservative estimates.

16.1 FLS Loads

As mentioned in chapter 3.2, load history for DLC 1.3 will be used, instead of DLC 1.2. The loads are taken from Frøyd's memo (Appendix, A), where he has calculated loads acting in the center of the hub (figure 6). These loads do not include waves or hydrodynamic loads. He has followed IEC 61400-1, with 3600 s simulation time of 4-30 m/s wind speeds (production wind speed from table 2.1). The loads from this memo are shown graphically with number of occurrence in one year.

Since load-time history graphs does not exist, a mean value of the load is found for each order of magnitude. This was done for each force and moment so a series of different amplitude loading could be made, see table 11.

Table 11: Calculated mean FLS loads

Load amplitude	n, 1 year	n, 20 years	F_x [kN]	F_y [kN]	F_z [kN]	M_x [MNm]	M_y [MNm]	M_z [MNm]
A	$9 \cdot 10^1$	$1.8 \cdot 10^3$	700	245	295	4.3	17.1	15.75
B	$9 \cdot 10^2$	$1.8 \cdot 10^4$	690	205	245	4.2	15.1	14.5
C	$9 \cdot 10^3$	$1.8 \cdot 10^5$	615	160	195	3.7	12.9	12.85
D	$9 \cdot 10^4$	$1.8 \cdot 10^6$	515	120	145	2.5	9.9	9.85
E	$9 \cdot 10^5$	$1.8 \cdot 10^7$	315	80	100	1.25	6.5	6.5
F	$9 \cdot 10^6$	$1.8 \cdot 10^8$	100	45	55	0.55	3.5	3.5

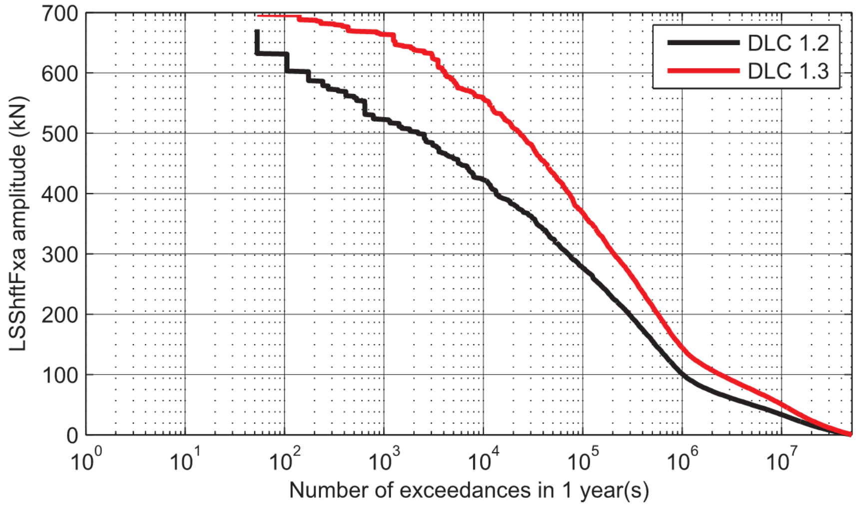

Figure 25: Force in x-direction, other graphs shown in appendix A

16.2 Stress Amplitude

Since load-time history graphs does not exist, an alternative way of finding stress amplitudes were established. Because of the load/stress relation, simulation for reference loads can be performed and peak stresses caused by the reference load defined. Ratio values between each reference load and the caused peak stress in a critical area can be found:

$$r = \frac{\sigma_{max}}{F}$$

After the r-values for each load in the critical areas has been calculated, they can be used to identify the stress amplitude in these areas. Since the time of when the different loads in table 11 are applied varies, there are several ways of summing up the stress amplitudes caused by the different loads. First a conservative approach will be used and if this determines a critical lifetime, another method will be performed. This conservative approach says that all the loads (forces and moments in x, y and, z direction) appear at the same time, therefore the stresses caused by the different loads will be summed up resulting in the highest possible stress amplitude.

The load factor (γ_f) is equal to 1 in FLS according to IEC 61400-1 and therefore the loads from table 11 could be used directly for the calculation of the stress amplitude.

A reference load of 100 kN was chosen for the forces, F and 5 MNm for the moments, M. The loads were applied to the hub and the contact surface between the bed plate, nose part and tower part were used as a reference surface, in order to apply the loads according to the reference coordinate system(figure 6).

The moments had to be converted in order to be applied on the hub. M_x was divided by the distance from center of the hub to the rotor blade connection and then applied here. My and Mz were divided by the distance from center to the hole in the front of the hub and applied to a spider connection here, see figure 26.

Table 12: Unit loads used in FLS simulation, see figure 26

Simulation	Load name	Load applied	Unit
Mean stress, σ_m	G_rotor1 and 2, G_stator, Gravitiy(1)	338.45+338.45+ 2256.3	kN
F_x	Fx=100kN	100	kN
F_y	Fy=100kN	100	kN
F_z	Fz=100kN	100	kN
M_x	Mx1, Mx2, Mx3=5kNm	$3 \cdot 700.28$	kN
M_y	My=5kNm	1913.5	kNm
M_z	Mz=5kNm	1913.5	kNm

The gravity forces from the rotor and stator were applied on the bed plate, nose part and the global z-axis was used as reference for the direction. The weight of the rotor and stator are gathered from table 2.1 and multiplied by the $\gamma_n = 1.15$.

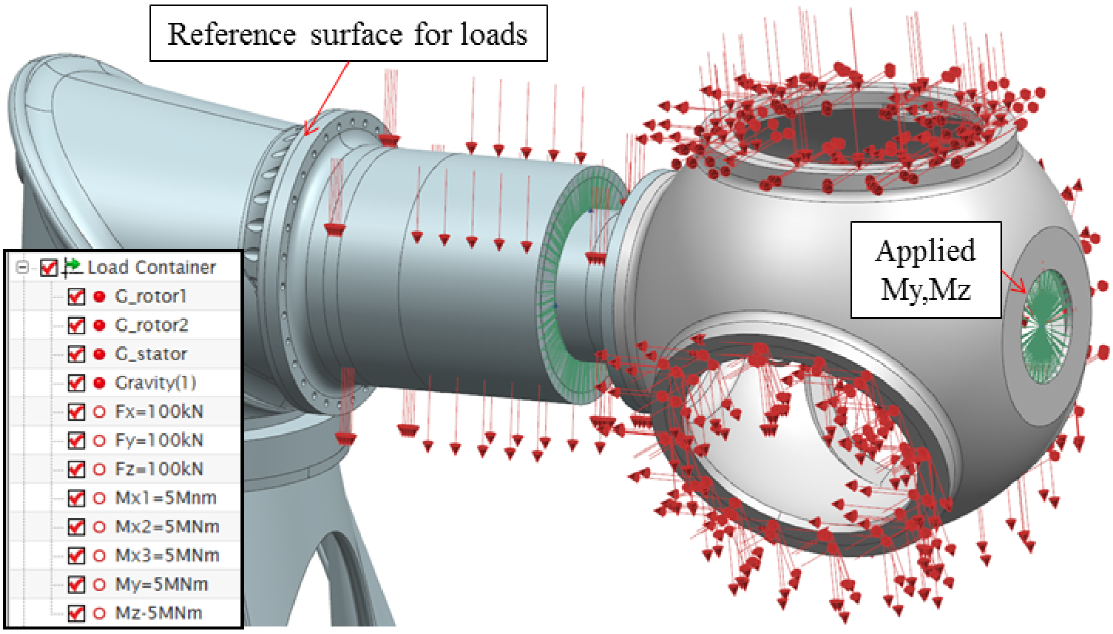

Figure 26: Unit loads used in FLS analysis

16.3 Meshing

The same mesh size is used as in Singh Klair's model on the hub, main shaft and bed plate. For yaw bearing (YB) and transition piece the mesh size from the ULS analysis in part I is used, see table 9.4. Figure 27 shows the whole FE model for the FLS analysis. All the mesh sizes used are displayed in table 16.3, where BP equals bed plate and YB yaw bearing.

Table 13: Mesh size for FLS simulation

Part	Size [mm]
Hub	500
Main Shaft	500
BP, Nose Part	325
BP, Tower Part	192
YB, Inner ring	255
YB, Outer ring	416
YB, Bearing rings	50
Transition piece	263
Tower	211

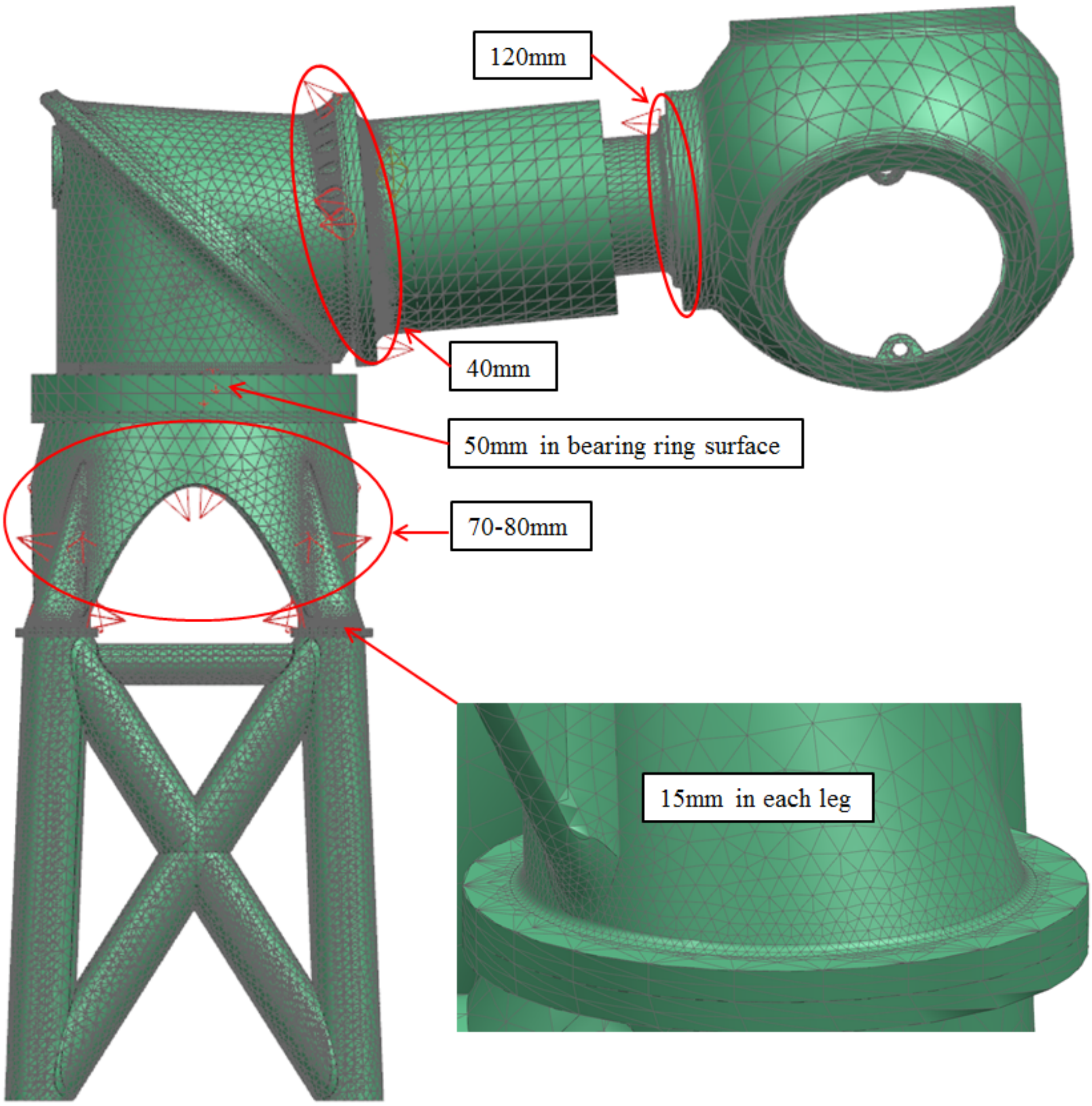

Figure 27: Meshed FLS model with mesh refinement ares

16.4 Boundary Conditions

The main shaft bearings consist of one front fixed bearing (double-row tapered roller bearing, TDO) and a back floating bearing [7]. The front bearing handles therefore forces in every direction (x, y and, z). M_y and M_z are handled by both the front and back bearing and M_x is supposed to rotate the generator and then transfer the moment on the outside of the nose part of the bed plate. Since the generator design is missing, a conservative assumption is made: All degrees of freedom (DOFs) are taken by the front bearing.

To simulate this, a manual coupling constrain was made in NX, between the outer surface of the front bearing attached to the main shaft and the outer surface of the bed plate, see figure 28. This function allows the center nodes in the spider attached to the bed plate and the one attached to the main shaft (front bearing) to share DOF's. Nastran could only handle this sharing of DOF's if AUTOMPC is enabled in the solution parameters.

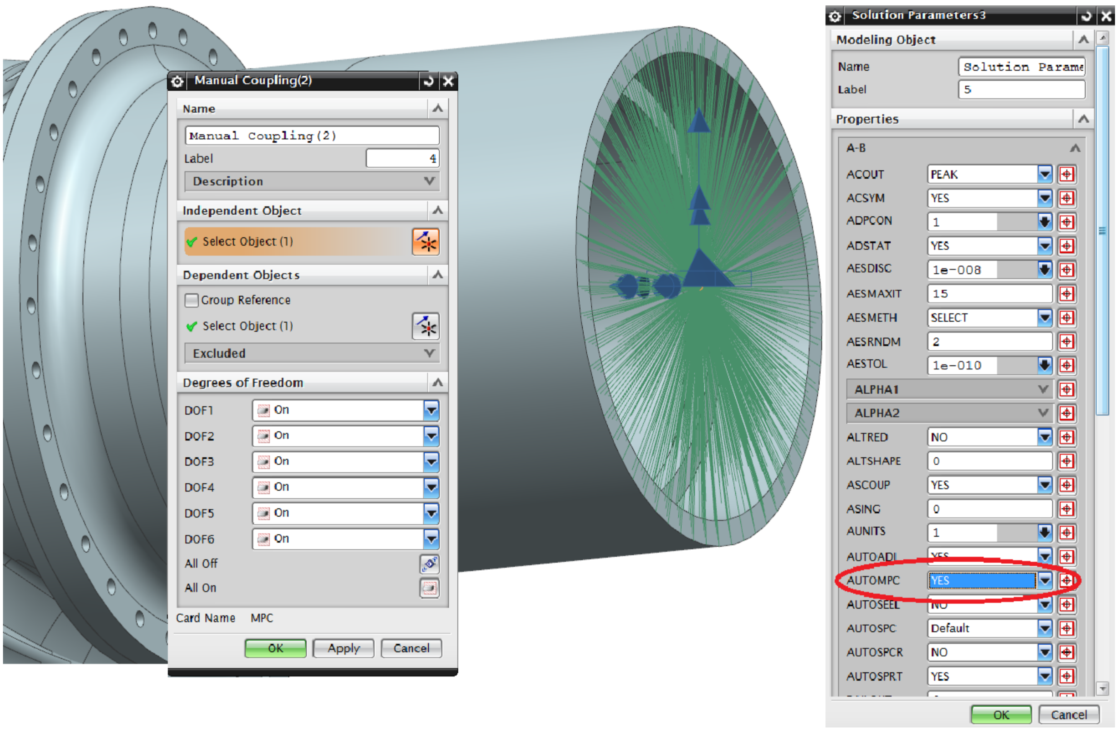

Figure 28: Manual coupling constrain and enabled AUTOMPC

The contact surfaces were glued as in the ULS simulation in chapter 11, also for the yaw bearing because of problems mentioned in chapter 11.2.2. For the added components there was set up an combination of gliding and glued contact, see figure 29

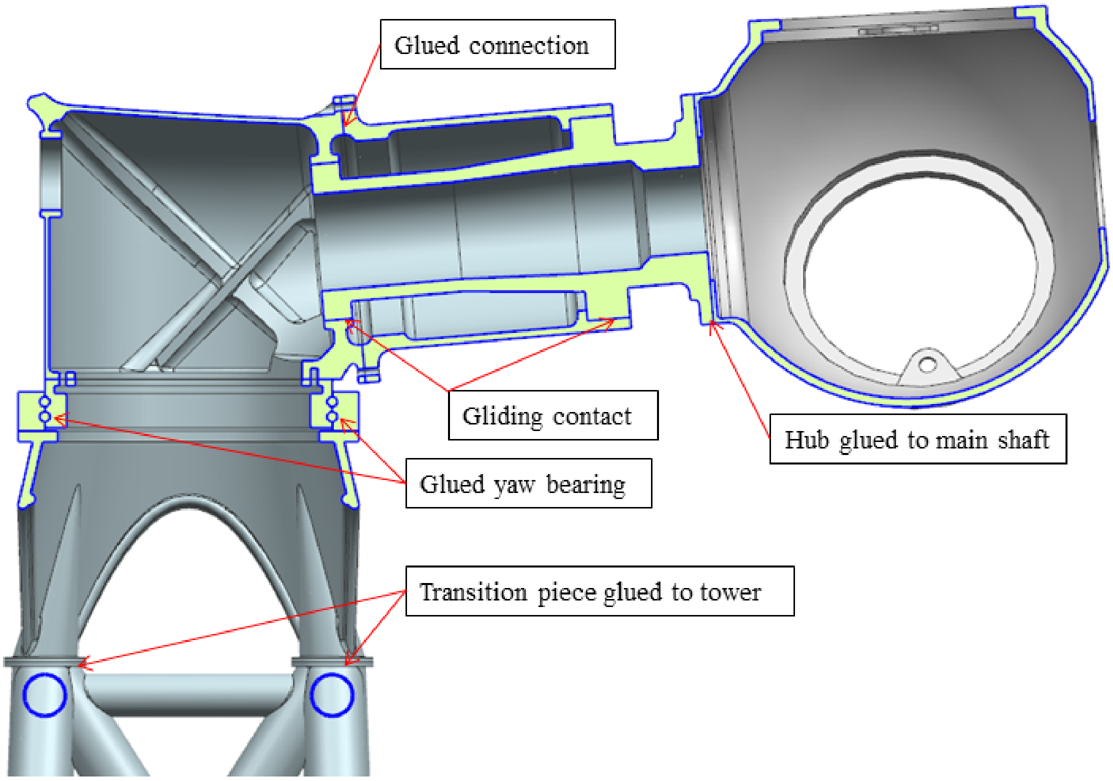

Figure 29: Contact surfaces in the FLS model

17 Fatigue Results

This fatigue analysis has created a large set of calculations and results. For submitting of the lifetime results for each part, the following procedure is used:

- First a figure showing mean stress results and the section view location used later are presented.
- Then simulation results for each reference load is presented in a table. A section view that displays most of the critical areas is chosen.
- A table of the critical areas calculated for fatigue and their r-values is submitted. The most critical area is highlighted in bold text.
- The values used to calculate the allowable number of cycles and damage for the applied loads are presented in a table.
- The total damage for the part is calculated and the lifetime presented.

The stress values for the fatigue results have been picked from the von-Mises results in NX with the "identify results" function. Critical areas in each component were identified, and stress values from each reference load were put in a table (see appendix B). From these stresses a set of ratio values for each load can be found as described in chapter 16.1.

The stress amplitude (σ_{eq}) for each load are calculated as a conservative approach as described in chapter 16.2. It is the sum of the forces and moments in each direction, times their r-value:

$$\sigma_{eq} = (F_x \cdot r_{Fx}) + (F_y \cdot r_{Fy}) + (F_z \cdot r_{Fz}) + (M_x \cdot r_{Mx}) + (M_y \cdot r_{My}) + (M_z \cdot r_{My})$$

The stresses from the critical areas have been picked from a relatively large area (not just a few elements) to favour a conservative assumption.

17.1 Main Shaft

The critical areas for fatigue in the main shaft were all located in the flange against the connection to the hub. There were also high stresses located around the cylinders simulating the bearings (see figure 30). They are only added to the model for load distribution and will not be included in the calculations.

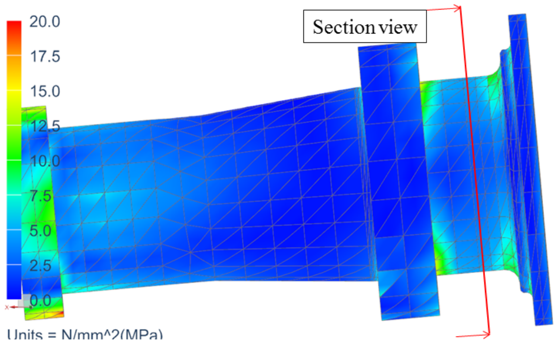

Figure 30: Mean stress results with section view location, in Main Shaft

	Direction		
Load	X	Y	Z
Force	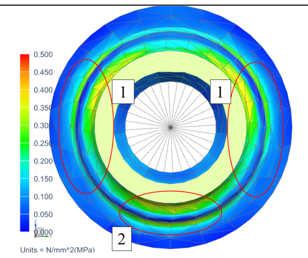	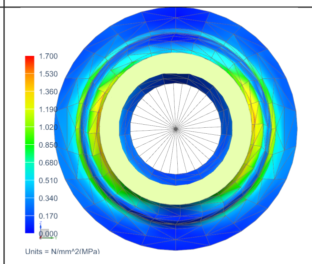	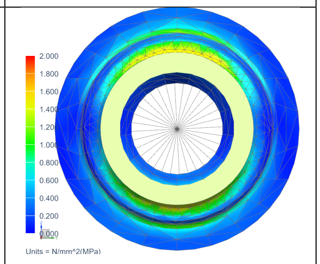
Moment	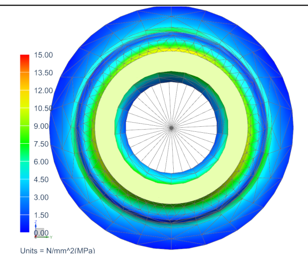	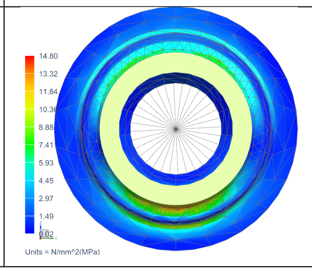	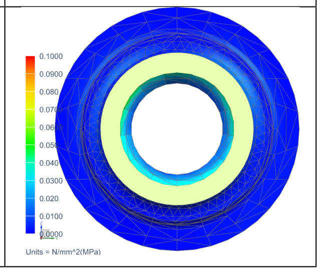

Point	Critical Areas	$\bar{\sigma}_m$	r_{Fx}	r_{Fy}	r_{Fz}	r_{Mx}	r_{My}	r_{Mz}
1	Side	3	0.005	0.016	0.003	2.24	0.5	0
2	**Bottom**	**11.9**	**0.005**	**0.007**	**0.02**	**2.24**	**2.98**	**0**

Load	n - Total	$\bar{\sigma}_m$	σ_{eq}	S_f	$\Delta\sigma R$	N	d
A	$1.8 \cdot 10^3$	11.9	59.3	1.44	207.0	$3.4 \cdot 10^7$	$5.3 \cdot 10^{-5}$
B	$1.8 \cdot 10^4$	11.9	51.2	1.59	203.6	$4.0 \cdot 10^7$	$4.5 \cdot 10^{-4}$
C	$1.8 \cdot 10^5$	11.9	43.2	1.77	194.6	$6.3 \cdot 10^7$	$2.8 \cdot 10^{-3}$
D	$1.8 \cdot 10^6$	11.9	31.9	1.95	158.3[a]	∞	0
E	$1.8 \cdot 10^7$	11.9	19.9	2.0	105.4[a]	∞	0
F	$1.8 \cdot 10^8$	11.9	9.6	2.25	61.1[a]	∞	0

Then the total damage of the main shaft after 20 years is:

$$D = \sum d = 5.3 \cdot 10^{-5} + 4.5 \cdot 10^{-4} + 2.8 \cdot 10^{-3} = \mathbf{3.3 \cdot 10^{-3}}$$

This equals a lifetime of:

$$\frac{20 \text{ years}}{D} = 5988 \text{ years (infinite lifetime)}$$

17.2 Bed Plate, Nose Part

Here the critical areas where found in the flange against the tower part of the bed plate and right front of this flange for the F_z and M_x loads:

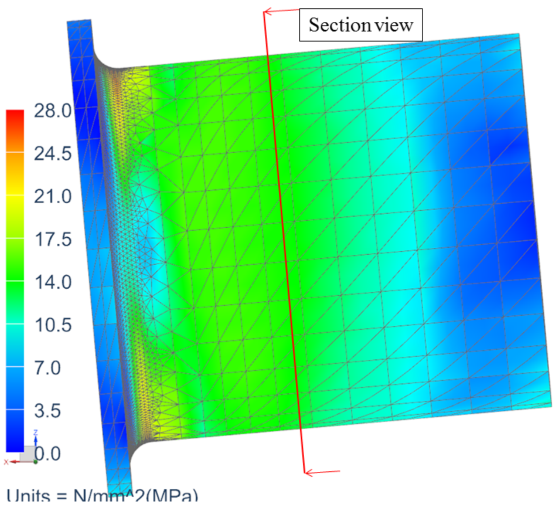

Figure 31: Mean stress results with section view location, in Bed Plate-Nose Part

[a] $\Delta\sigma R < \Delta\sigma_w$ which means that the stress amplitude is "assumed as non-damaging in fatigue" according to EN 13445-6.

	Direction		
Load	X	Y	Z
Force	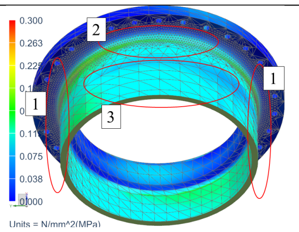	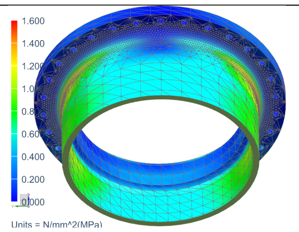	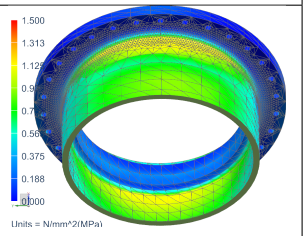
Moment	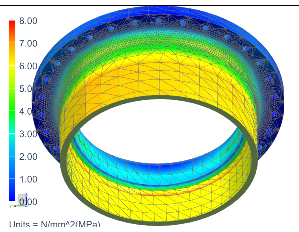	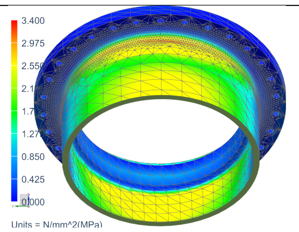	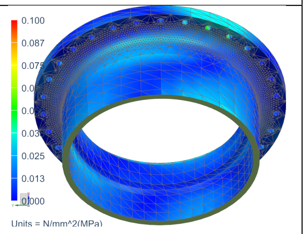

Point	Critical Areas	$\bar{\sigma}_m$	r_{Fx}	r_{Fy}	r_{Fz}	r_{Mx}	r_{My}	r_{Mz}
0	Whole flange	0	0.002	0	0	0	0	0
1	Both sides	11	0.002	0.015	0.007	1.08	0.14	0
2	**Top/Bottom**	**28**	**0.002**	**0.01**	**0.014**	**1.08**	**0.68**	**0**
3	Front of flange	15	0.002	0.01	0.01	1.6	0.5	0

Load	n - Total	$\bar{\sigma}_m$	σ_{eq}	S_f	$\Delta\sigma R$	N	d
A	$1.8 \cdot 10^3$	28	20.5	1.46	70.8[a]	∞	0
B	$1.8 \cdot 10^4$	28	17.7	1.61	69.7[a]	∞	0
C	$1.8 \cdot 10^5$	28	15.1	1.81	67.9[a]	∞	0
D	$1.8 \cdot 10^6$	28	11.2	1.99	54.9[a]	∞	0
E	$1.8 \cdot 10^7$	28	7.2	2.07	37.2[a]	∞	0
F	$1.8 \cdot 10^8$	28	3.7	2.34	22.2[a]	∞	0

Then the total damage of the bed plate, nose part after 20 years is:

$$D = \sum d = 0$$

This equals a infinite lifetime.

[a] $\Delta\sigma R < \Delta\sigma_w$ which means that the stress amplitude is "assumed as non-damaging in fatigue" according to EN 13445-6.

17.3 Bed Plate, Tower Part

There were found several critical areas in the bed plate, tower part and Inside1 were considered as the most critical. The stresses in this point are mostly caused by coarse mesh since the peak stress only appeared in a few nodes.

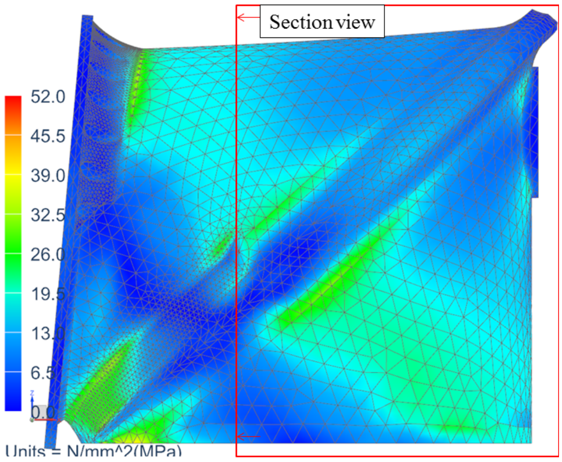

Figure 32: Mean stress results with section view location, in Bed Plate-Tower Part

	Direction		
Load	X	Y	Z
Force	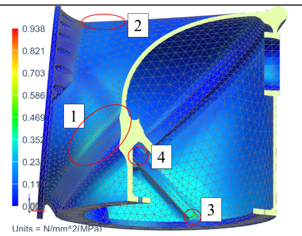	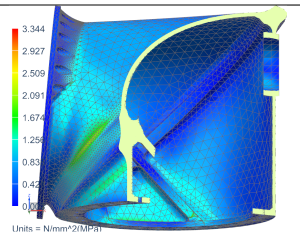	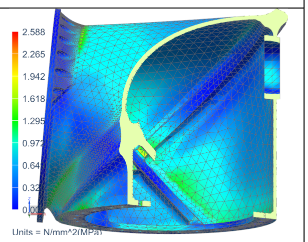
Moment	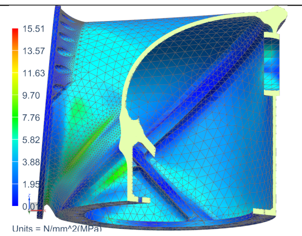	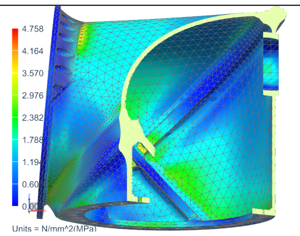	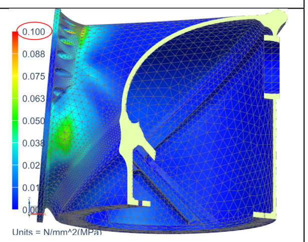

Point	Critical Areas	$\bar{\sigma}_m$	r_{Fx}	r_{Fy}	r_{Fz}	r_{Mx}	r_{My}	r_{Mz}
1	Both sides	33	0.003	0.023	0.015	2.04	0.64	0
2	Top	35	0.002	0.009	0.017	0.94	0.74	0
3	**Inside1**	33.2	**0.01**	**0.034**	**0.017**	**1.66**	**0.68**	**0**
4	Inside2	**52**	0.004	0.007	0.022	1.26	0.96	0

Name	n - Total	$\bar{\sigma}_m$	σ_{eg}	S_f	$\Delta\sigma R$	N	d
A	$1.8 \cdot 10^3$	52	33.4	1.49	116.2[a]	∞	0
B	$1.8 \cdot 10^4$	52	28.9	1.65	116.1[a]	∞	0
C	$1.8 \cdot 10^5$	52	25.2	1.86	116.6[a]	∞	0
D	$1.8 \cdot 10^6$	52	18.8	2.07	92.5[a]	∞	0
E	$1.8 \cdot 10^7$	52	12.0	2.17	66.9[a]	∞	0
F	$1.8 \cdot 10^8$	52	6.2	2.49	39.6[a]	∞	0

Then the total damage of the bed plate, tower part after 20 years is:

$$D = \sum d = 0$$

This equals an infinite lifetime.

17.4 Transition Piece

Since the nacelle turn on top of the transition piece a peak stress that appear in on leg could appear in another leg next time the load appear. With that in mind the critical areas found in each leg were assumed to appear in just one leg. It means that every leg has the same critical point at the same place (see figure 34).

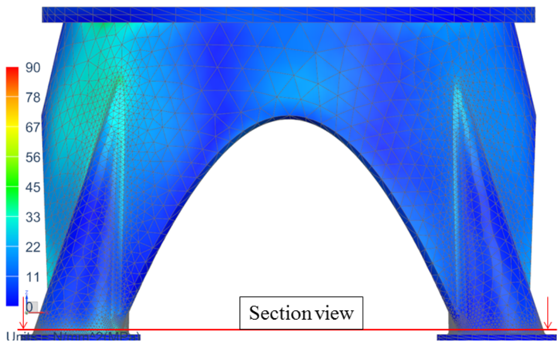

Figure 33: Mean stress results with section view location, in transition piece

Point	Critical Areas	$\bar{\sigma}_m$	r_{Fx}	r_{Fy}	r_{Fz}	r_{Mx}	r_{My}	r_{Mz}
1	Towards center	**90**	0.01	0.017	0.029	2.64	0.9	0
2	**Right stiffener**	85	**0.017**	**0.027**	**0.029**	**2.72**	**1.1**	**0**

[a] $\Delta\sigma R < \Delta\sigma_w$ which means that the stress amplitude is "assumed as non-damaging in fatigue" according to EN 13445-6.

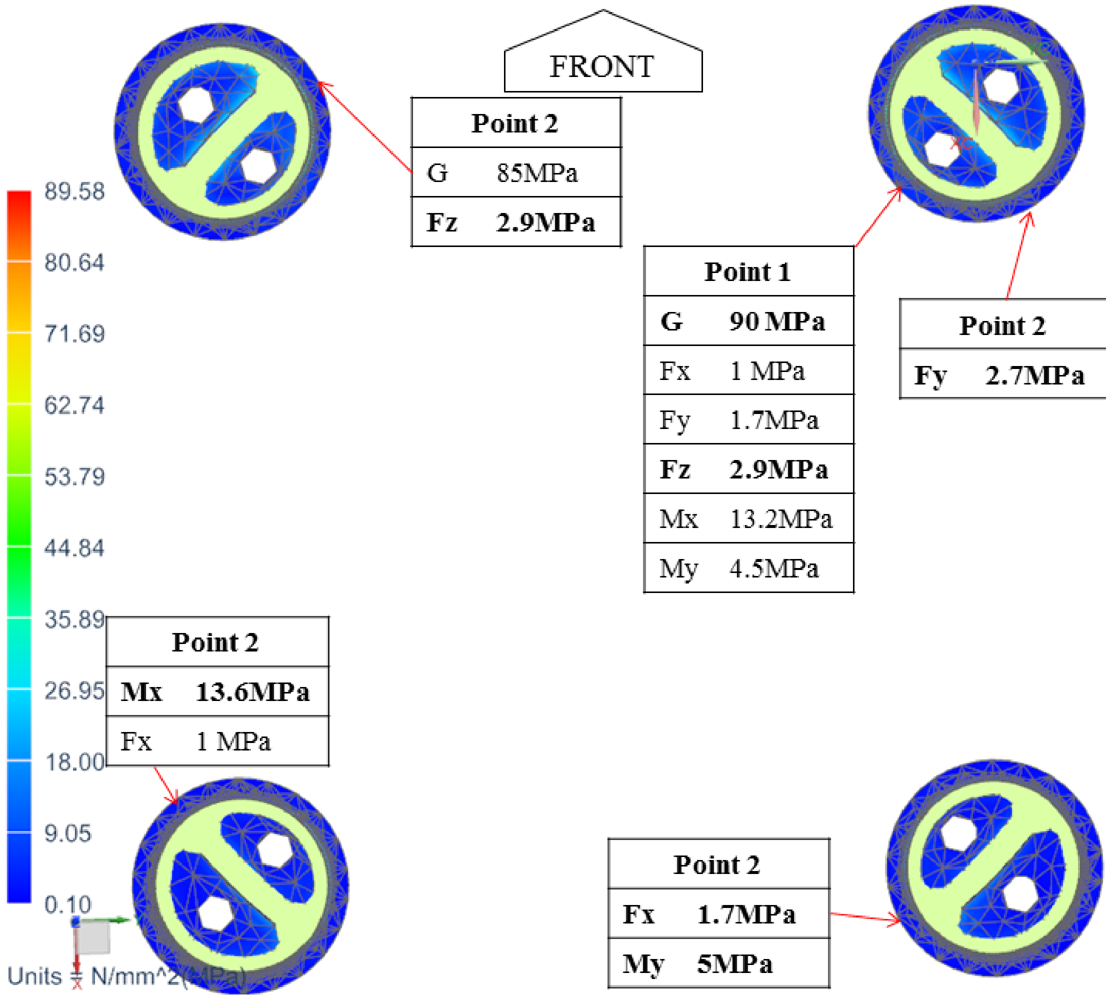

Figure 34: FLS results for transition piece, section view from above

Name	n - Total	$\bar{\sigma}_m$	σ_{eq}	S_f	$\Delta\sigma R$	N	d
A	$1.8 \cdot 10^3$	90	49.3	1.53	176.1[a]	∞	0
B	$1.8 \cdot 10^4$	90	42.9	1.71	179.1[a]	∞	0
C	$1.8 \cdot 10^5$	90	36.7	1.95	179.4[a]	∞	0
D	$1.8 \cdot 10^6$	90	27.2	2.21	142.5[a]	∞	0
E	$1.8 \cdot 10^7$	90	17.0	2.37	104.3[a]	∞	0
F	$1.8 \cdot 10^8$	90	8.5	2.69	58.2[a]	∞	0

[a] $\Delta\sigma R < \Delta\sigma_w$ which means that the stress amplitude is "assumed as non-damaging in fatigue" according to EN 13445-6.

Then the total damage of the bed plate, tower part after 20 years is:

$$D = \sum d = 0$$

This equals an infinite lifetime.

17.5 Discussion

It is only the main shaft where $\Delta\sigma R$ is higher than the fatigue limit,$\Delta\sigma_w$ at 186 MPa (see figure 24). Here it is load C that creates most damage to the main shaft. This means that loads that occur between 10^3 and 10^4 times a year are the most crucial loads for the lifetime.

As mentioned in chapter 16.2 another approach for the stress amplitude (σ_{eq}) would be established if the results revealed a critical lifetime. Since a infinite lifetime was found it is no need for a new calculation of σ_{eq}.

The total damage equals infinite lifetime for all the parts ($>$ 5988 years) but a rough calculation of critical load for the main shaft (see appendix E) reveals that if load D is increased by a factor of 2.2 it may cause a lifetime near 20 years for the main shaft.

Another surprising result is that moment about the z-axis (M_z) do almost nothing to fatigue since it caused almost zero stresses in all the components (less than 0.1 MPa with the reference load, M_z = 100 kN).

From the r-values it seems that moment about the x-axis (M_x) is the most critical moment because it gives the highest r-values.

18 Conclusion

The assignment was to do mechanical design and dimensioning of yaw bearing and a transition piece between the bed plate and tower. Yaw bearing simulations are difficult to perform, some design changes were done and the displacement in the connection flange was found to be ok. There were also made room for mounting brakes and yaw motors for operation of the wind turbine.

Several transition piece concepts was developed, and a final design is recommended. This is concept 2, the short cone presented for tower section 1. There are still areas with stresses above the calculated maximum stress of 218 MPa and a few elements with stresses above the yield strength (peak stress of 262 MPa). However the applied loads, have a 50 year occurrence period which is much longer than the designed lifetime of 20 years. Therefore yielding in small areas with that loading is believed to be ok. Alternatively the stronger material EN-GJS-500-7, with a calculated max. stress of 264 MPa could be used for the transition piece. With this material the stress, weight, and standard requirements are fulfilled.

The other part of the assignment was to verify the lifetime of 20 years by doing a fatigue analysis of the hub, main shaft and bed plate. Since the loads were applied directly on the hub, it could cause incorrect results for the hub. So the hub was not included the fatigue analysis, but the transition piece was included instead. The calculations verified all the parts for a lifetime over 20 years, despite several conservative assumptions. In fact, only the main shaft that was exposed to stresses above the fatigue limit. This analysis revealed a lifetime greater than 5988 years for all the parts. Which again are strengthening the suggestion of that some yielding is ok, for the ultimate load cases (in part 1). However a doubled amplitude stress will increase the damage drastically, so the safety factor against a lifetime of 20 years is not as high as it seems.

With this thesis NOWITECH are one step closer to a finished design of a 10 MW offshore reference turbine. The main parts except the generator (rotor and stator) have now been designed.

19 Further Work

The proposals for further work are:

- Establish the other design load cases for fatigue design, mentioned in chapter 3.2 (2.4 (failure), 3.1 (start up), 4.1 (normal shut down) and 6.4 (parked)) and perform a FLS analysis with these loads.
- Perform a dynamic simulation in FEDEM windpower with different wind speeds to verify the amplitude stresses and results. With the same model FLS analysis of the hub could also be established.
- Use the same FEDEM model to simulate extreme wind conditions to verify the ULS results.
- Do a proper calculation of all the bolt connections for dimensioning of the bolt sizes.
- Find solutions for different yaw motors and brakes.

References

[1] Lars Frøyd. Six dof hub forces and bending moments from ultimate and fatigue load case simulations of version 2 of the 10 mw rotor. 2012.

[2] Google. 2013. `https://maps.google.no/maps?q=lat+53.22+lon+3.22\&ie=UTF-8\&ei=zXpvUufNFY6rhAf-roGoBg\&ved=0CAoQ_AUoAg`.

[3] Erich Hau. Wind turbines - fundamentals, technologies, application, economics. (3), 2012.

[4] Wikipedia. Wind turbines. October 2013. `http://en.wikipedia.org/wiki/Wind_turbine`.

[5] World Wind Energy Association. October 2013. `http://www.wwindea.org/home/index.php`.

[6] Mohammad Akram Khan. Design of rotor hub for nowiterch 10 mw reference wind turbine, 2012.

[7] Ebbe Berge Smith. Design av nacelle for en 10mw vindturbin. ntnu, 2012.

[8] Sandeep Singh Klair. Design of nacelle and rotor hub for nowitech 10mw reference turbine. ntnu, 2013.

[9] Gunnar Härkegård. *Dimensjonering av maskindeler.* 2004.

[10] Norman E. Dowling. *Mechanical Behavior of Materials, Engineering Methods for Deformation, Fracture and Fatigue.* 2013.

[11] The International Electrotechnical Commission. Iec 61400-1. 2007.

[12] Lars Frøyd. *Wind turbine design: evaluation of dynamic loads on large offshore wind turbines.* PhD thesis, 2012.

[13] DNV. Dnv-ds-j102, design and manufacture of wind turbine blades. October 2010.

Appendix

A HUB Loads for Structural Design [1]

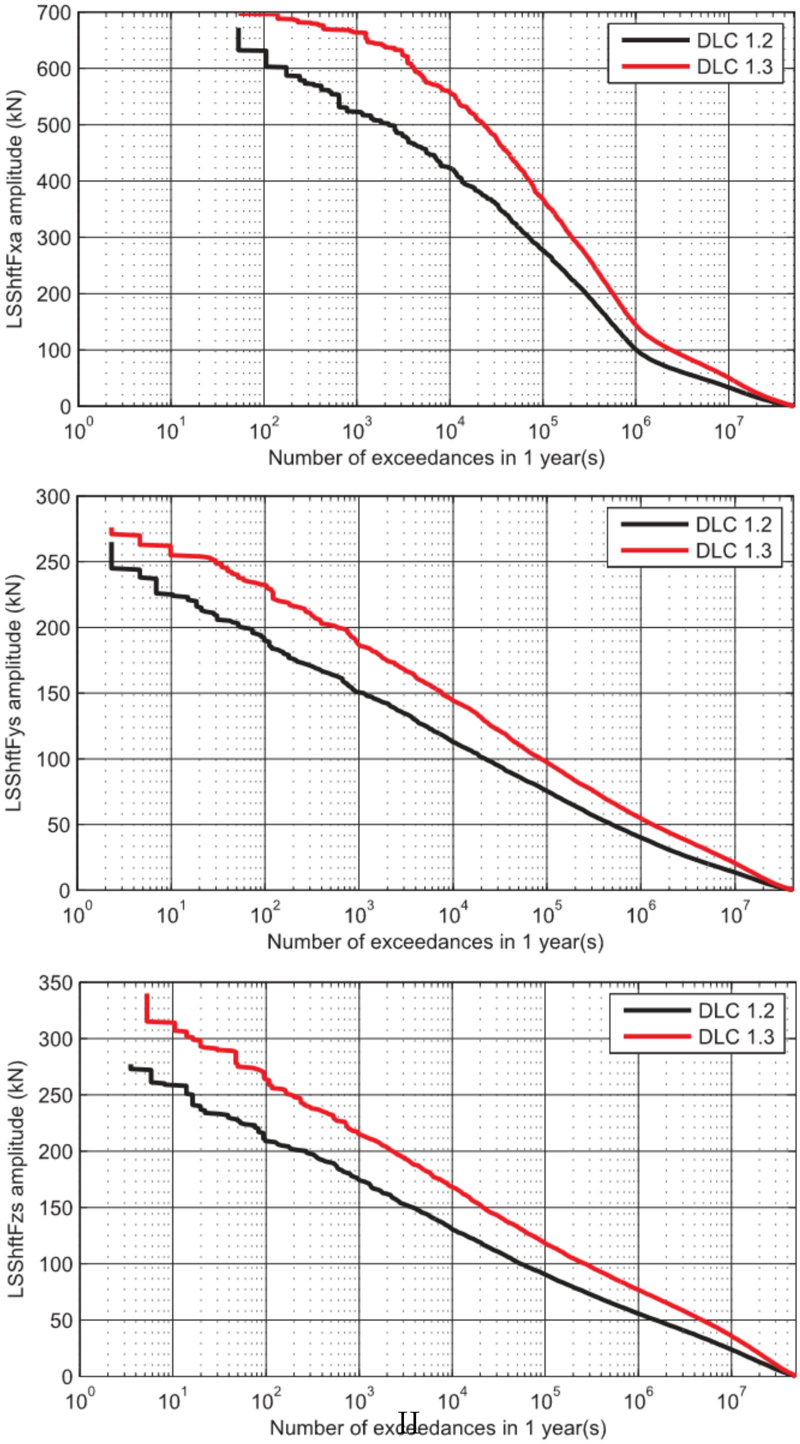

Figure 2: Probability of exceedance of hub force amplitudes. Following FAST notation.

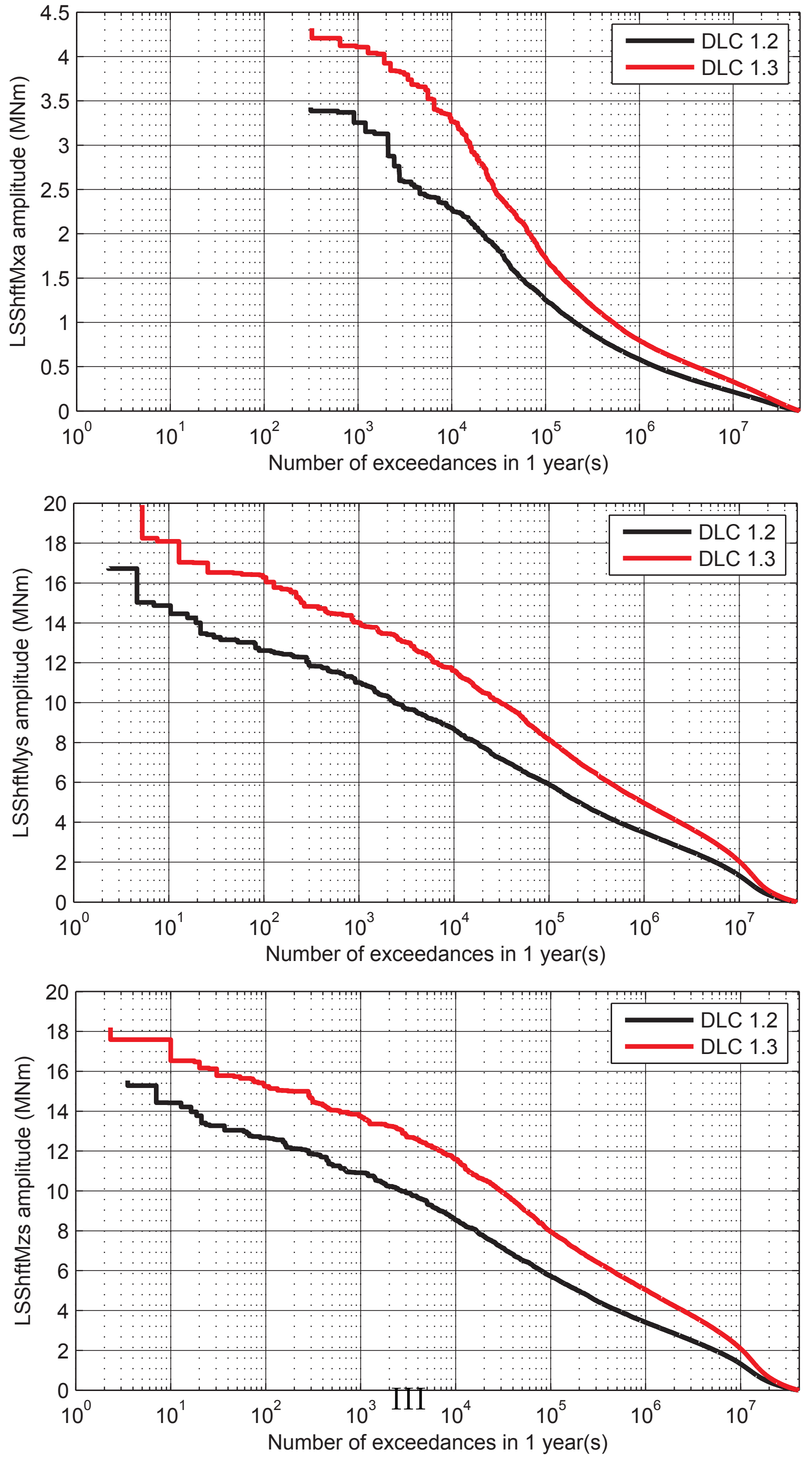

Figure 3: Probability of exceedance of hub moment amplitudes. Following FAST notation.

B Measured Peak Stresses and Calculated r-values

Main Shaft

	Point	Check point	Gravity	Fx=	Fy=	Fz=	Mx=	My=	Mz=
				100kN	100kN	100kN	5MNm	5MNm	5MNm
Unit load			σm	σ,Fx	σ,Fy	σ,Fz	σ,Mx	σ,My	σ,Mz
Fx		Hole flange							
Fy	1	Side	3	0,5	1,6	0,3	11,2	2,5	0
Fz	2	Bottom	11,9	0,5	0,7	2	11,2	14,9	0
Mx		Whole flange							
My	2	Bottom	11,9	0,5	0,7	2	11,2	14,9	0
Mz	-	-							0

Bed plate - Nose part

	Point	Check point	Gravity	Fx=	Fy=	Fz=	Mx=	My=	Mz=
				100kN	100kN	100kN	5MNm	5MNm	5MNm
Unit load			σm	σ,Fx	σ,Fy	σ,Fz	σ,Mx	σ,My	σ,Mz
Fx		Hole flange		0,2					
Fy	1	Both sides	11	0,2	1,5	0,7	5,4	0,7	0
Fz	2	Top/Bottom	27	0,2	1	1,4	5,4	3,4	0
Mx	3	Front of flange	15	0,2	1	1	8	2,5	0
My		Top/Bottom	27	0,2	1	1,4	5,4	3,4	0
Mz		-		0,2					

Bed plate - Tower part

	Point	Check point	Gravity	Fx=	Fy=	Fz=	Mx=	My=	Mz=
				100kN	100kN	100kN	5MNm	5MNm	5MNm
Unit load			σm	σ,Fx	σ,Fy	σ,Fz	σ,Mx	σ,My	σ,Mz
Fx	3	Inside1	33,2	1	3,4	1,7	8,3	3,4	>0,1
Fy	1	Both sides	33	0,3	2,3	1,5	10,2	3,2	>0,1
Fz	2	Top - inside/oustide	35	0,2	0,9	1,7	4,7	3,8	>0,1
Mx	1	Both sides	33	0,3	2,3	1,5	10,2	3,2	>0,1
My	2	Top		0,2	0,8	1,7	4,7	3,8	>0,1
Mz	4	Inside2	52	0,4	0,7	2,2	6,3	4,8	

Transition piece

	Point	Check point	Gravity	Fx=	Fy=	Fz=	Mx=	My=	Mz=
				100kN	100kN	100kN	5MNm	5MNm	5MNm
Unit load			σm	σ,Fx	σ,Fy	σ,Fz	σ,Mx	σ,My	σ,Mz
Fx		Right back leg inside	48	1,7	1,7	2,5	7,3	5	
Fy		Inside bw front legs	42	0	2,6	1,5	6,4	2	
Fz		Right front leg inside	90	1,7	2,7	2,9	8,2	4	
Mx		Left back leg front	15	0,6	1,6	1,1	13,6	2,7	
My		Right back leg inside	48	1,7	1,6	2,5	7,3	5	
Mz	1	Towards center	90	1	1,7	2,9	13,2	4,5	0
	2	To the right	85	1,7	2,7	2,9	13,6	5,5	0

Main Shaft

Point	Where	Gravity						
		σm	r,Fx	r,Fy	r,Fz	r,Mx	r,My	r,Mz
	Whole Flange	**0**	0	0	0	0	0	0
1	Side	**3**	0,005	0,016	0,003	2,24	0,5	0
2	Bottom	**11,9**	0,005	0,007	0,02	2,24	2,98	0
	Whole Flange	**0**	0	0	0	0	0	0
2	Bottom	**11,9**	0,005	0,007	0,02	2,24	2,98	0
		0	0	0	0	0	0	0

Bed plate - Nose part

Point	Where	Gravity						
		σm	r,Fx	r,Fy	r,Fz	r,Mx	r,My	r,Mz
0	Hole flange	**0**	0,002	0	0	0	0	0
1	Both sides	**11**	0,002	0,015	0,007	1,08	0,14	0
2	Top/Bottom	**28**	0,002	0,01	0,014	1,08	0,68	0
3	Front of flange	**15**	0,002	0,01	0,01	1,6	0,5	0
0	Top/Bottom	**28**	0,002	0,01	0,014	1,08	0,68	0
0	-	**0**	0,002	0	0	0	0	0

Bed plate - tower part

Point	Where	Gravity						
		σm	r,Fx	r,Fy	r,Fz	r,Mx	r,My	r,Mz
3	Inside1	**33,2**	0,01	0,034	0,017	1,66	0,68	0
1	Both sides	**33**	0,003	0,023	0,015	2,04	0,64	0
2	Top - inside/oustide	**35**	0,002	0,009	0,017	0,94	0,76	0
1	Both sides	**33**	0,003	0,023	0,015	2,04	0,64	0
2	Top	**0**	0,002	0,008	0,017	0,94	0,76	0
4	Inside2	**52**	0,004	0,007	0,022	1,26	0,96	0

Transition piece

Point	Where	Gravity						
		σm	r,Fx	r,Fy	r,Fz	r,Mx	r,My	r,Mz
6	Right back leg inside	**48**	0,017	0,017	0,025	1,46	1	0
3	Inside bw front legs	**42**	0	0,026	0,015	1,28	0,4	0
4	Right front leg inside	89	0,017	0,027	0,029	1,64	0,8	0
5	Left back leg front	**15**	0,006	0,016	0,011	2,72	0,54	0
6	Right back leg inside	**48**	0,017	0,016	0,025	1,46	1	0
1	Towards center	**90**	0,01	0,017	0,029	2,64	0,9	0
2	To the right	**85**	0,017	0,027	0,029	2,72	1,1	0

C Result of gliding contact in yaw bearing

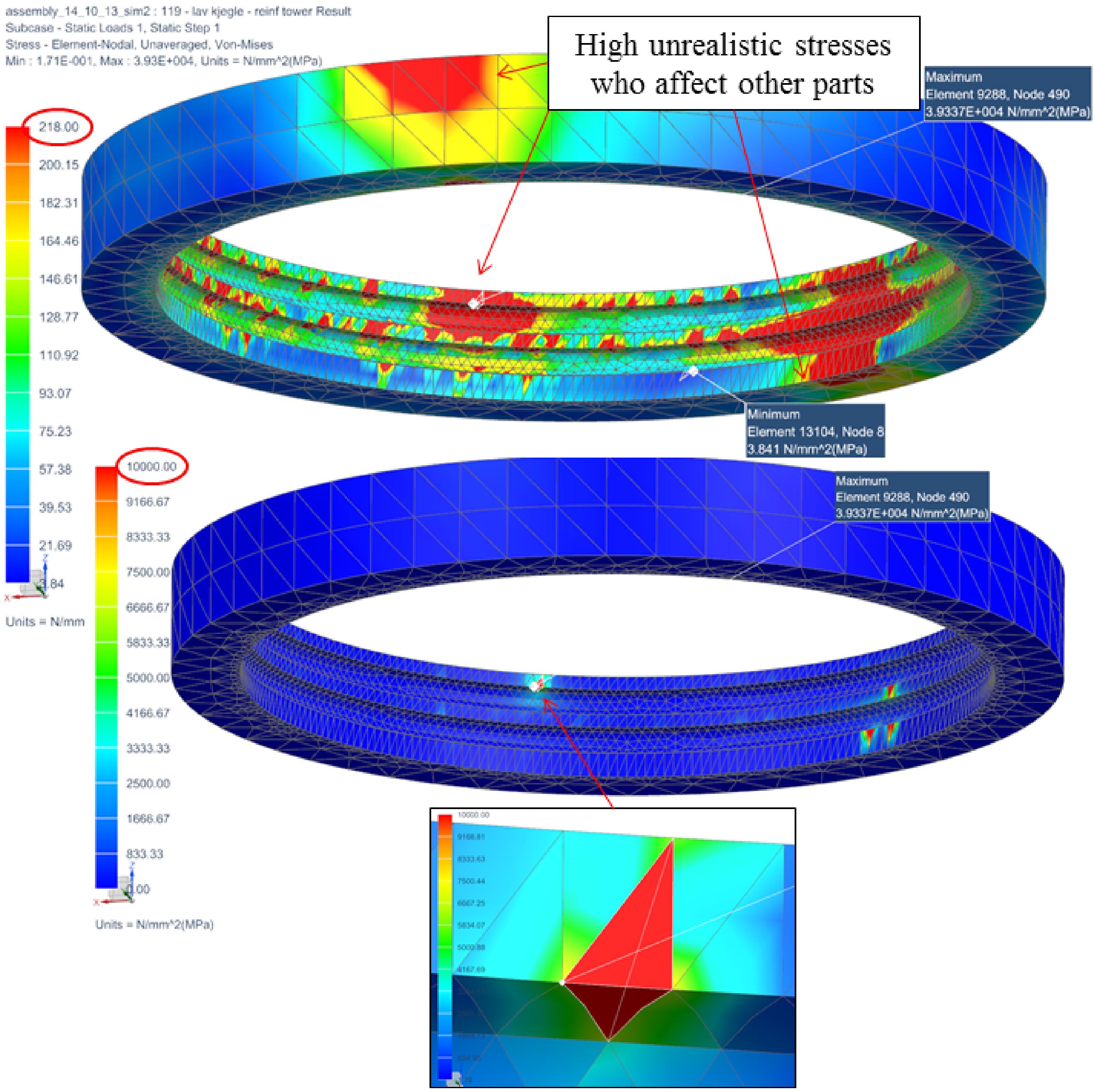

D Results from concept 1

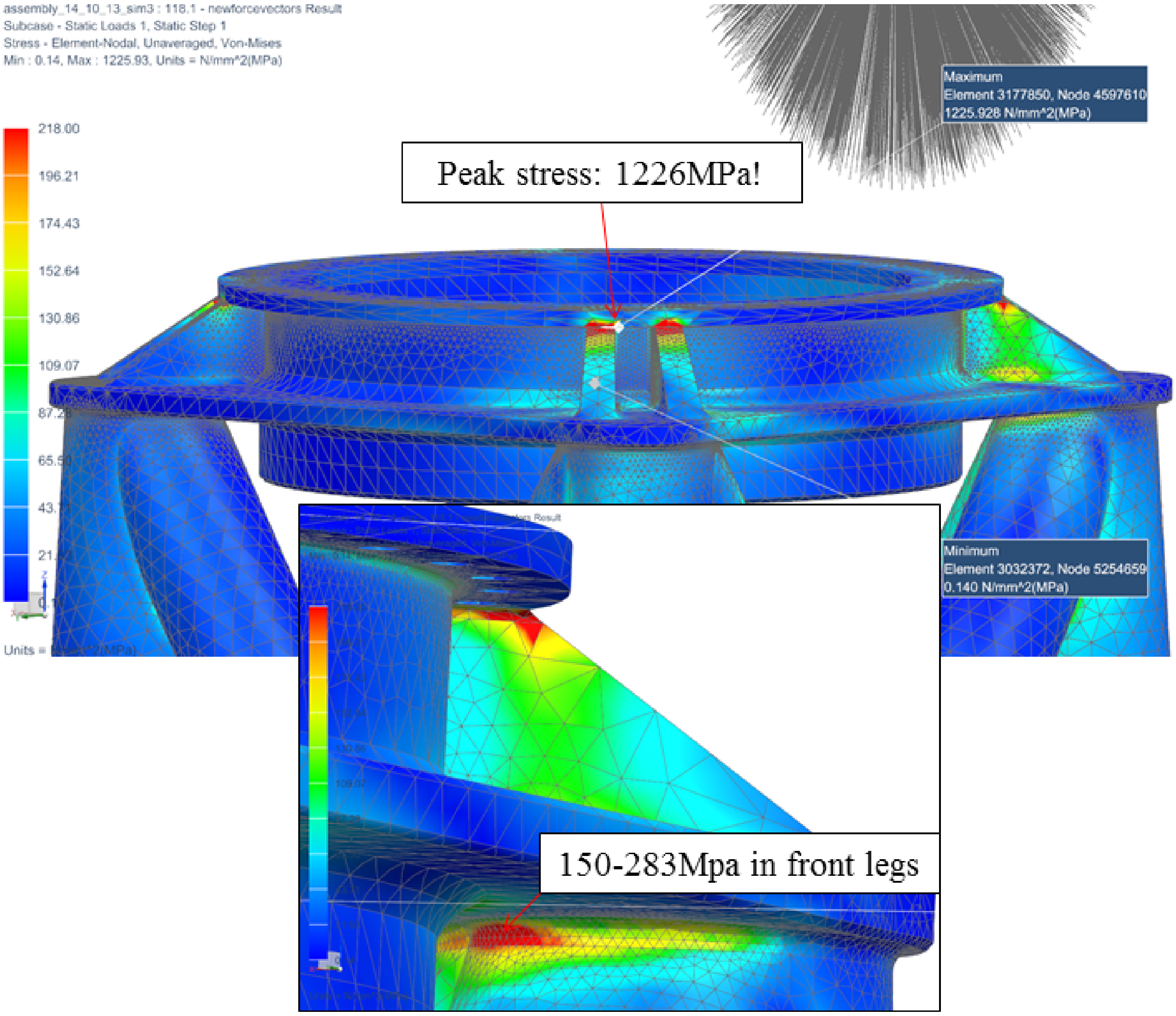

E Rough Estimation of Critical Load

Backwards calculation for main shaft:

$$N = \frac{n}{d} = \frac{1.8 \cdot 10^6}{0.5} = 3.6 \cdot 10^6$$

the $\Delta\sigma R$ value in the SN-curve (figure 24) with this N is $275MPa$. This equals a amplitude stress, σ_{eq} of:

$$\frac{\Delta\sigma R}{2 \cdot S_f} = \frac{275MPa}{2 \cdot 1.95} = 70.5MPa$$

This rough estimation show us that the FLS loads have to be 2.2 times greater or more before the main shaft approaches a critical lifetime:

$$\frac{70.5MPa}{31.9MPa} = 2.2$$